SANDIA REPORT
SAND2014-0831
Unlimited Release
Printed February 3, 2014

Nuclear Fuel Cycle System Simulation Tool Based on High-Fidelity Component Modeling

David E. Ames II

Prepared by
Sandia National Laboratories
Albuquerque, New Mexico 87185 and Livermore, California 94550

Sandia National Laboratories is a multi-program laboratory managed and operated by Sandia Corporation, a wholly owned subsidiary of Lockheed Martin Corporation, for the U.S. Department of Energy's National Nuclear Security Administration under contract DE-AC04-94AL85000.

Issued by Sandia National Laboratories, operated for the United States Department of Energy by Sandia Corporation.

Available to DOE and DOE contractors from
U.S. Department of Energy
Office of Scientific and Technical Information
P.O. Box 62
Oak Ridge, TN 37831

Telephone: (865) 576-8401
Facsimile: (865) 576-5728
E-Mail: reports@adonis.osti.gov
Online ordering: http://www.osti.gov/bridge

Available to the public from
U.S. Department of Commerce
National Technical Information Service
5285 Port Royal Rd.
Springfield, VA 22161

Telephone: (800) 553-6847
Facsimile: (703) 605-6900
E-Mail: orders@ntis.fedworld.gov
Online order: http://www.ntis.gov/help/ordermethods.asp?loc=7-4-0#online

SAND2014-0831
Unlimited Release
Printed February 3, 2014

Nuclear Fuel Cycle Simulation Tool Based on High-Fidelity Component Modeling

David E. Ames
Advanced Nuclear Concepts
Sandia National Laboratories
P.O. Box 5800
Albuquerque, New Mexico 87123-1136

Abstract

The DOE is currently directing extensive research into developing fuel cycle technologies that will enable the safe, secure, economic, and sustainable expansion of nuclear energy. The task is formidable considering the numerous fuel cycle options, the large dynamic systems that each represent, and the necessity to accurately predict their behavior. The path to successfully develop and implement an advanced fuel cycle is highly dependent on the modeling capabilities and simulation tools available for performing useful relevant analysis to assist stakeholders in decision making. Therefore a high-fidelity fuel cycle simulation tool that performs system analysis, including uncertainty quantification and optimization was developed. The resulting simulator also includes the capability to calculate environmental impact measures for individual components and the system.

An integrated system method and analysis approach that provides consistent and comprehensive evaluations of advanced fuel cycles was developed. A general approach was utilized allowing for the system to be modified in order to provide analysis for other systems with similar attributes. By utilizing this approach, the framework for simulating many different fuel cycle options is provided. Two example fuel cycle configurations were developed to take advantage of used fuel recycling and transmutation capabilities in waste management scenarios leading to minimized waste inventories.

INTENTIONALLY LEFT BLANK

CONTENTS

FIGURES

TABLES

NOMENCLATURE

ABR	Advanced Burner Reactor
AFCI	Advanced Fuel Cycle Initiative
ANL	Argonne National Laboratory
AP1000	Westinghouse Electric Company Reactor
BOC	Beginning of Cycle
CAIN	CAlculation of INventory of Spent Fuel
DOE	U.S. Department of Energy
DU	Depleted Uranium
EFPD	Effective Full Power Days
ENDF/B	Evaluated Nuclear Data Files – Basic
EOC	End of Cycle
FC1	Fuel Cycle example 1
FC2	Fuel Cycle example 2
FP	Fission Products
GDP	Gross Domestic Product
Gen-IV	Generation IV Nuclear Fuel Systems
GIF	Generation IV International Forum
HDI	Human Development Index
HLW	High Level Waste
HTGR	High Temperature Gas Reactor
HTR	High Temperature Reactor
HTTR	High Temperature Test Reactor
IAEA	International Atomic Energy Agency
IFBA	Integral Fuel Burnable Absorber
INL	Idaho National Laboratory
JAERI	Japan Atomic Energy Research Institute
LEU	Low Enriched Uranium
LLW	Low Level Waste
LWR	Light Water Reactor
MCNP	Monte Carlo N – Particle
MCNPX	Monte Carlo N – Particle Extended
MT	Metric Tons
MTU	Metric Tons of Uranium
NFCSS	Nuclear Fuel Cycle Simulation System
NGNP	Next Generation Nuclear Plant
NRC	Nuclear Regulatory Commission
ORNL	Oak Ridge National Laboratory
PWR	Pressurized Water Reactor
PYREX	Discrete Burnable Absorber Rods
SCALE	Standardized Computer Analysis for Licensing Evaluation
SFR	Sodium Fast-cooled Reactor
SWU	Separative Work Unit
tIHM	Ton Initial Heavy Metal

TRISO	Tri-structural Isotropic
TRU	Transuranic Isotopes (Np, Pu, Am, Cm)
UNDP	United Nations Development Program
UREX	URanium EXtraction
VHTR	Very High Temperature Reactor

INTENTIONALLY LEFT BLANK

1 INTRODUCTION

Energy consumption per capita is one of the single most important factors in regards to living standards of individuals across the world. Studies have continually shown an indisputable link between energy consumption and individuals overall well-being [1].

The Human Development Index (HDI) is considered to the best and most comprehensive measure for quality of life. It incorporates factors such as life expectancy, education, income inequality, poverty rates, and Gross Domestic Product (GDP) per capita [2]. The index is normalized to give a value between zero and one, with one representing the highest possible standard of living or most developed country, and zero being the least. Countries that score an HDI greater than 0.79 are considered to have a "very high human development," while those with values between 0.67 and 0.79 are rated as having an "high human development," and those with values between 0.48 and 0.67 are "medium human development", and below 0.48 are classified as having a "low human development."

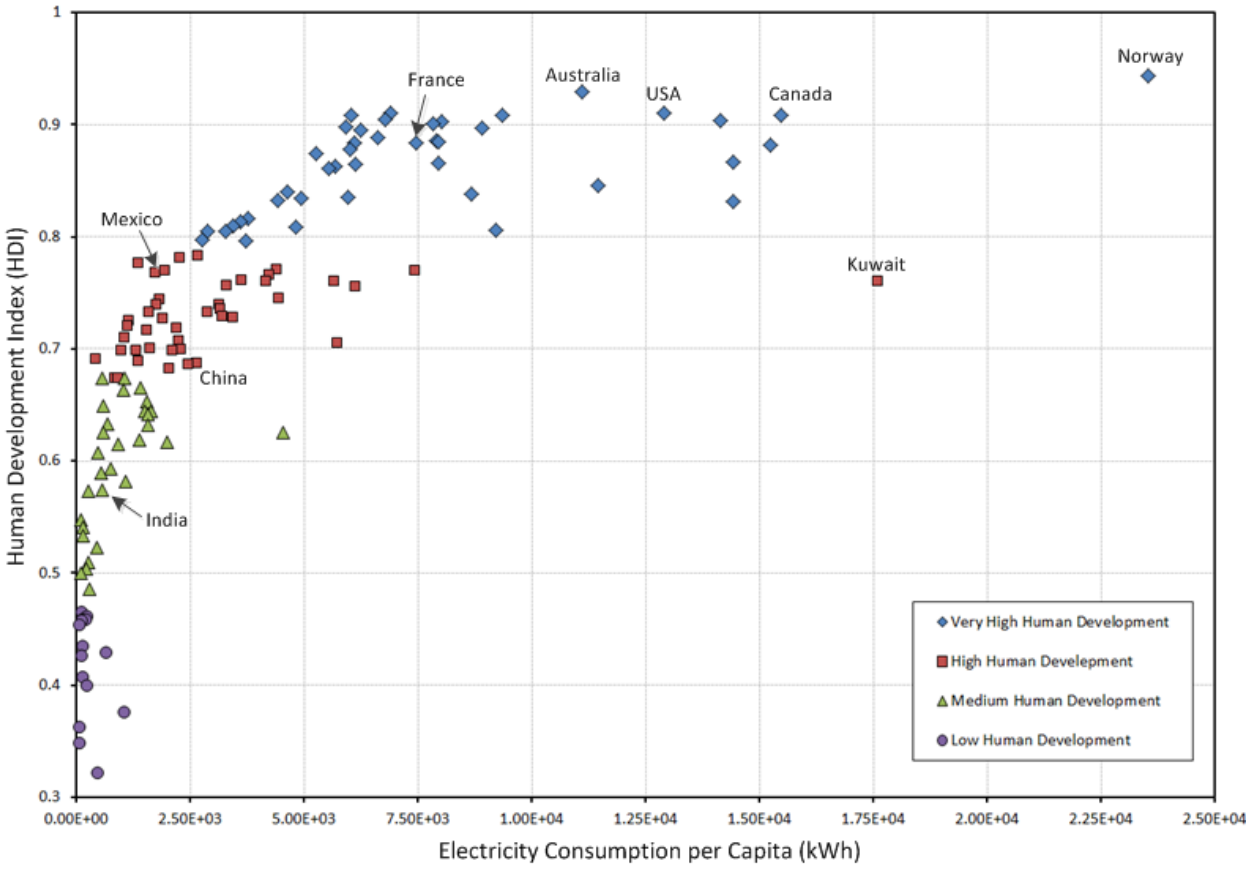

Figure 1.1. HDI and Electricity Consumption per Capita (2013).

As shown in Figure 1.1, Norway has the highest HDI at 0.955, while Niger ranks lowest at 0.304. The USA has an HDI of 0.937 and is ranked number 3 overall. The results overwhelmingly show that the greater the energy consumption per capita for a community, the greater the standard of living (HDI) for those individuals. Consequently, energy consumption can be used as an indicator for the overall wellbeing of a society and for a comparison between different societies around the globe. As expected, all nations strive to increase their HDI standing. The most effective and straightforward way to accomplish this is by adding energy generation capacity. Of particular notice is China and India, the two most populated countries in world (35% of the world's population), which are striving to rapidly increase their HDI, and will have a huge impact on overall energy needs worldwide.

Figure 1.2 displays HDI data and Carbon Dioxide (CO_2) emissions for 180 countries. The trend indicates that along with high HDI values comes greater CO_2 emissions. Just like energy's link to quality of life, energy is also intricately entwined with the environment. Much of the global-scale environmental degradation seen today is attributed to the adverse effects of energy production and use. Thus, nations are faced with the struggle to increase energy generation in order to provide a higher standard of living for their citizens, but must also do so in an environmentally responsible way.

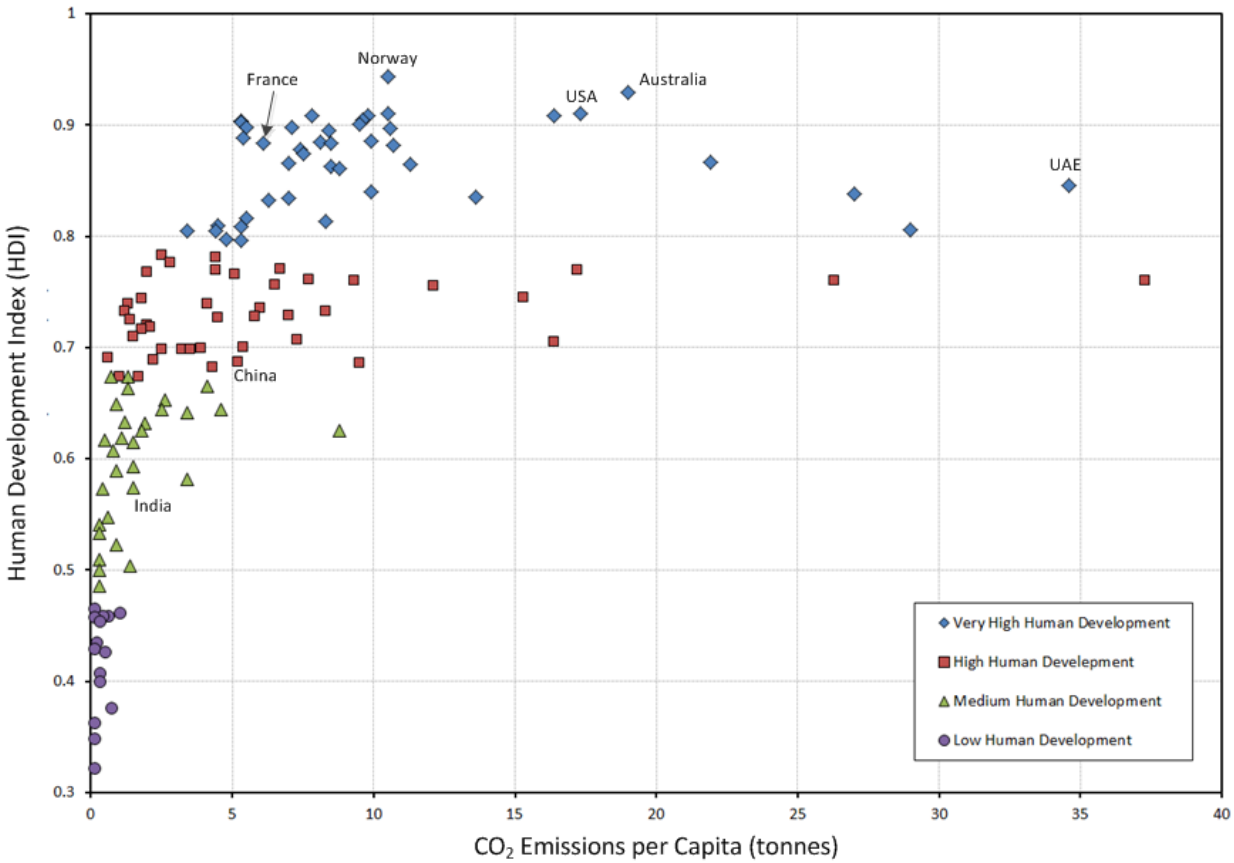

Figure 1.2. HDI vs. CO_2 Emissions per Capita (2013).

Of recent the world has become much more sensitive to the relationship between energy and the environment. In so much, nations and groups of nations have proposed and/or implemented policies [2, 3] to mitigate the harmful environmental effects associated with energy generation. Important goals and basic principles of future energy sources include: 1) reducing greenhouse gas emissions, 2) minimizing the overall environmental footprint, 3) safety and reliability, 4) sustainability, 5) economics, 6) efficiency, and 7) energy independence.

Nuclear energy is arguably one of the best sources for electricity generation that can meet these future needs and requirements. Even so, advances and improvements must be made for nuclear energy to be competitive in the future. The presented research addresses the above principles with emphasis on environmental aspects by means of developing a modeling approach for advanced nuclear energy systems that minimize high level waste inventories while at the same time maximizing fuel utilization and providing a secure energy source.

1.1 The Nuclear Fuel Cycle

The various activities associated with the production of electricity from nuclear reactions are referred to collectively as the nuclear fuel cycle. It includes a comprehensive collection of components that are linked together for the main purpose of generating electricity by means of nuclear power. It includes everything from the exploration for uranium deposits, to harnessing the energy released during fission, to the disposal of radioactive waste. The nuclear fuel cycle can be thought of as the progression of nuclear fuel through a series of differing stages. There are three major parts to the cycle: 1) Front-end, 2) In-core, and 3) Back-end.

The front-end of the fuel cycle begins with the exploration of uranium deposits. The uranium ore is extracted by various mining methods. Conventional techniques such as open pit and underground mining are most commonly used. Next the mined uranium ore is processed and treated to extract the uranium through the milling process. The milled uranium is then converted to a form that can be used by commercial facilities to enrich the fissile component by either gaseous diffusion or gas centrifuge enrichment technologies. The last step for the front-end is fuel fabrication, where enriched fuel is converted to a final usable fuel form and incased in a protective cladding for service in nuclear reactors.

The in-core or service period of the fuel cycle makes up the second major category of the fuel cycle. This part of the fuel cycle is concerned with fuel performance while in the reactor core. Much emphasis is placed on fuel management strategies, irradiation effects on the fuel, fuel cladding interactions, and radioactivity release during normal use and accidents. The reactor type, neutron spectrum, and fuel type are important parameters for the service period.

The back-end of the fuel cycle begins when the fuel is discharged from the reactor. Upon removal, the fuel is stored onsite temporarily and then prepared for either permanent storage or for reprocessing. The decision of whether to recycle the used reactor fuel or to place it directly into storage greatly affects the makeup of the back-end of the fuel cycle. Waste management is the key issue with this part of the fuel cycle.

1.1.1 Fuel Cycle Technologies

The United States Department of Energy (DOE) established the Fuel Cycle Technologies (FCT) program to focus on the research and development needed to maximize performance and safety of the existing nuclear fleet, while also developing advanced systems for the future that will ensure nuclear energy's continued role as a clean and sustainable energy source. The FCT program is envisioned to support the growth of nuclear power and enable energy independence in the U.S. by developing and demonstrating technologies that facilitate the transition to a stable, long-term, environmentally, economically, and politically acceptable advanced fuel cycle. The main goals of the FCT are to reduce high-level waste volume, greatly reduce long-lived and highly radiotoxic elements, and reclaim valuable energy content of spent nuclear fuel. In part, the FCT program seeks to:

- Strengthen the technical and scientific basis for extended storage of used nuclear fuel (UNF) and high-level waste (HLW), and work with industry to develop and demonstrate solutions.
- Identify and test options to enhance accident tolerance of the current reactor fleet.
- Identify and select preferred fuel cycle options that address key challenges, including deployment of advanced uranium enrichment technologies to enhance national energy security.
- Deploy the selected extended storage solution while developing the scientific basis for permanent disposal options in a geologic repository.
- Demonstrate and deploy the selected enhancements for accident tolerance.
- Conduct science-based, engineering-driven research to fully evaluate and characterize the selected sustainable fuel cycle options.
- Implement safe strategies for management of UNF and HLW, including both storage and permanent disposal solutions.
- Deploy advanced nuclear systems for affordable, safe, and secure nuclear-generated electricity while continuing to test enabling technologies for future deployment.

To realize the full potential of the fuel cycle, advanced nuclear systems must be implemented. The Generation IV International Forum (GIF) focuses on future nuclear energy system concepts to meet the growing energy needs of the world. It is an international program coordinating research and working together to develop promising new nuclear energy systems. Attention is given to improving safety features, addressing nuclear nonproliferation and physical protection issues, optimizing natural resource utilization, minimizing waste, and being economically competitive with other energy generating systems. The GIF has selected six systems for further development. The systems are:

1) Gas-Cooled Fast Reactor,
2) Very High Temperature Reactor,
3) Supercritical Water Cooled Reactor,
4) Sodium Cooled Fast Reactor,
5) Lead Cooled Fast Reactor, and
6) Molten Salt Reactor.

As part of the Generation IV program the U.S. DOE has focused efforts on the Next Generation Nuclear Plant (NGNP). The NGNP program promotes research and development specific to the Very High Temperature Reactor (VHTR).

The VHTR is designed to be a high-efficiency energy system, which can supply electricity and process heat to a wide-range of high temperature and energy intensive applications. The VHTR is a passively safe design. The refractory core, low power density, and low excess reactivity enable this design feature. It is a graphite moderated gas-cooled reactor that supplies heat with core outlet temperatures equal to or greater than 850° Celsius, which enables applications such as hydrogen production, process heat for the petrochemical industry, or seawater desalination. The VHTR can be utilized in a deep-burn configuration to transmute problematic actinides and reduce the burden of HLW management.

The U.S. has also played a major role in the development of Sodium-cooled Fast Reactors (SFR). Fast spectrum systems offer a higher degree of flexibility when it comes to the transmutation process. They not only provide the ability to better control the isotopic makeup of the waste stream through nuclide destruction, but also the capability to fully utilize the available fuel resources with high conversion/breeding ratios. The FSR is primarily designed for actinide management and offers improved waste disposal and uranium utilization.

1.2 Procedures

1.2.1 Nuclear Fuel Cycle Setup

There are numerous options for nuclear fuel cycles. With the many different types of reactors, fuel types, reprocessing schemes, and fuel cycle component technologies the possible options become almost limitless. To demonstrate the simulation procedure two fuel cycle options were selected. Each has its own advantages and disadvantages, but they were selected to provide example cases. Both are arranged for minimization or elimination of high-level waste inventories, which is an essential component of publicly acceptable sustainable nuclear energy strategies [3].

The arrangement of fuel cycle example 1 (FC1) is depicted in Figure 1.3. The front-end (mining, milling, enrichment, and fuel fabrication) of the fuel cycle is shown in the top center and follows current practices incorporated and used in the once-through fuel cycle. The only difference is the availability of depleted uranium (DU) arising from the reprocessing step, allowing for the recycling of the uranium. The fuel elements then enter the reactor (AP1000) for power production. When the fuel is exhausted it is removed from the reactor and temporarily stored to allow the used fuel to cool down to the specified limits required before reprocessing can be performed. During reprocessing the fuel is separated into fission products (FP), uranium, and transuranics (TRU). The FP are conditioned and prepared for long-term high-level waste (HLW) storage. The uranium is stored as low-level waste (LLW) and is also available for recycle. The

TRU and uranium are fabricated into fuel elements for the SFR, which operates as an advanced burner reactor (ABR) with multiple reprocessing steps. After the final pass the fuel is removed from the ABR and it is considered HLW and sent to the designated facility for permanent HLW storage.

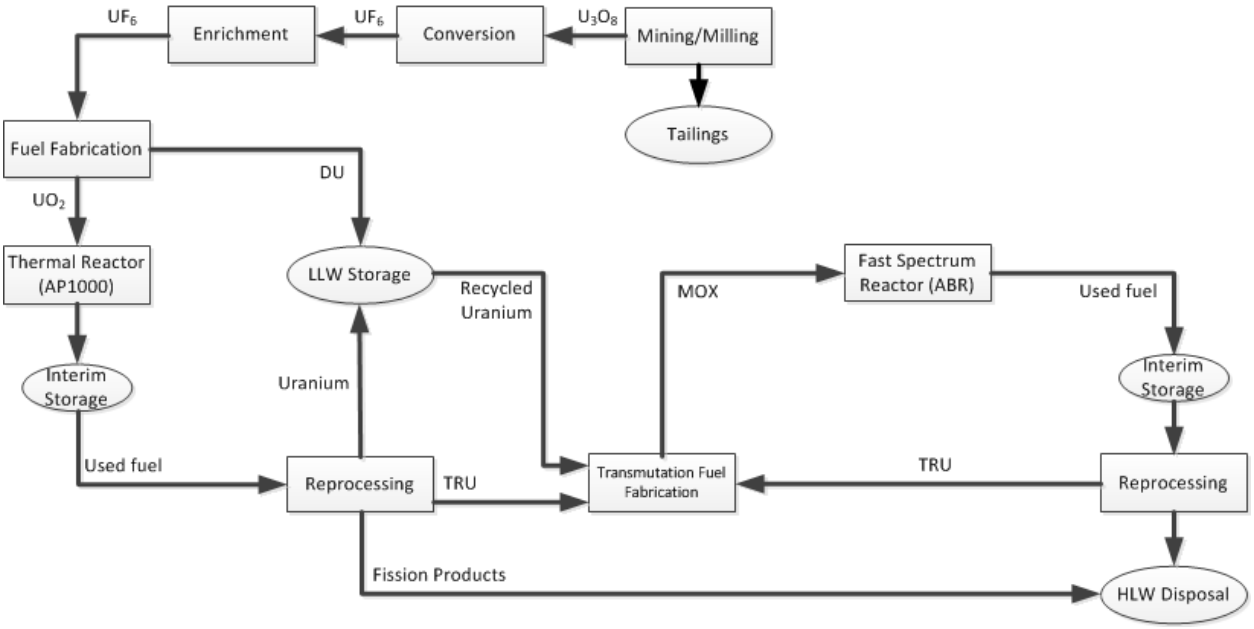

Figure 1.3. FC1 Arrangement.

The arrangement for fuel cycle example 2 (FC2) is shown in Figure 1.4. The front-end remains unchanged and the first reactor is again the AP1000. The used fuel from the AP1000 is separated into fission FP, uranium, and TRU. The FP are designated for long-term HLW storage. The uranium is stored as LLW and is also available for recycle. The TRU are fabricated into fuel elements to be recycled in the VHTR, which operates in an actinide burn mode without further reprocessing. After removal from the VHTR the used fuel is prepared for permanent HLW storage.

In each case the material is tracked throughout the system with emphasis on composition changes within the reactor systems, material streams during reprocessing, and the final effect on HLW waste management strategies. The representative models for the reactor systems and fuel cycle components are stand-alone units that also offer the ability to link each for the purpose of uncertainty quantification and optimization procedures.

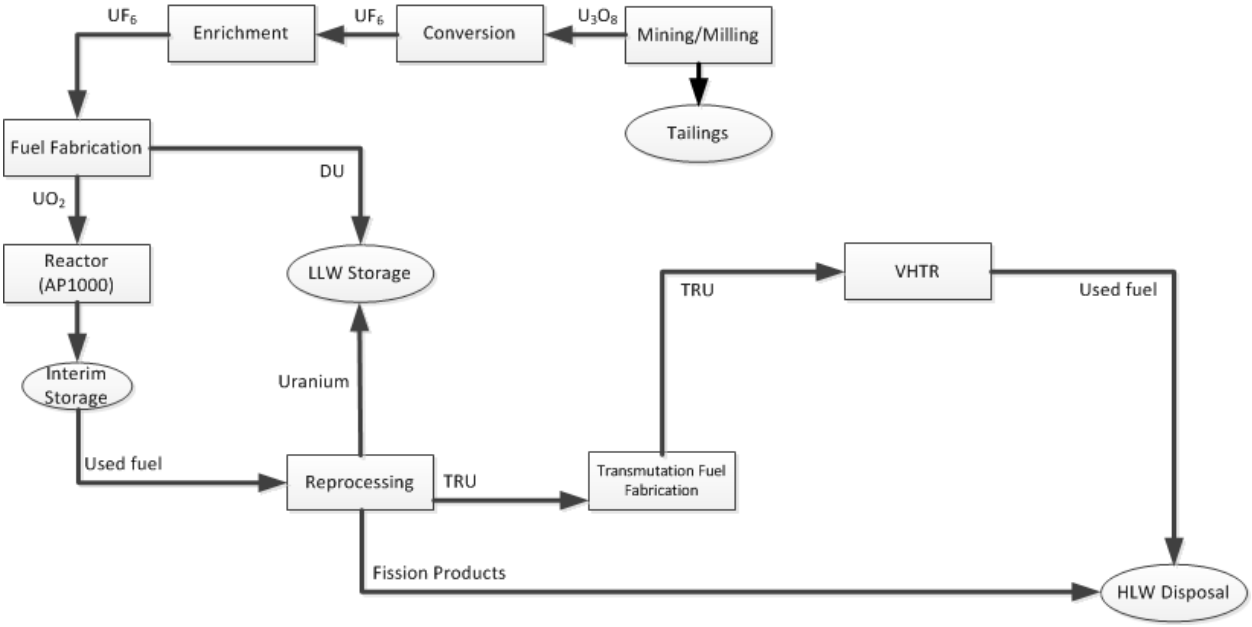

Figure 1.4. FC2 Arrangement.

2 APPLIED CODE SYSTEMS

Modeling and simulation play a critical role in modern scientific and technical endeavors. To the extent that scientific advances are dependent on their effective use. Modeling, theory, and simulation can enhance our understanding of known systems, provide qualitative and quantitative insights into experimental work, guide the choice of the experimental system to study, enable the design of new systems, provide quantitative results to replace experiments, and extend limited experimental data into new domains of parameter space [4]. Due to the difficulties of dealing with radioactive materials, modeling and simulation will play a critical role in advancing nuclear research programs.

2.1 Code Systems

State-of-the-art computer code systems were utilized to create realistic high fidelity 3D whole-core models representing the reactors and fuel cycle components. A collection of diverse code systems were selected based on their ability to meet the outlined research objectives and the capabilities and limitations accompanying each.

The Monte Carlo based code, MCNP, was heavily utilized for creating the 3D whole-core models representing the reactor units. Functional modules within the Standardized Computer Analysis for Licensing Evaluation (SCALE) code system were used to model the HLW facility and for 3D whole-core modeling. The front-end components and the integrated system were developed within the MATLAB/Simulink computational environment. In addition, the Nuclear Fuel Cycle Simulation System (NFCSS) was used for benchmarking front-end component models.

2.1.1 MCNP

Monte Carlo N-Particle (MCNP) is a general purpose code that can be used for neutron, photon, electron, or coupled neutron/photon/electron transport. MCNP is the internationally recognized code for analyzing the transport of neutrons and gamma rays, and is developed and maintained by Los Alamos National Laboratory.

MCNP5

MCNP is a code that is continuously undergoing development at Los Alamos national Laboratory and has periodic releases. MCNP5 is very versatile due to important standard features such as: multiple source description options, flexible tally structure, an extensive collection of cross section data, large collection of variance reduction techniques, and geometry and output tally plotters. Neutron energy ranges in MCNP5 are limited to that of 10^{-11} to 20 MeV [5, 6].

MCNPX

The code system MCNPX (Monte Carlo N-Particle eXtended) extends the capabilities of MCNP4C3 to nearly all particles, nearly all energies, and to nearly all applications without an additional computational time penalty. It is fully 3D and time dependent, and uses up to date nuclear cross section libraries and physics models for particle types and energies where tabular data are not available. MCNPX version 2.6.0 includes depletion/burnup/transmutation capability that is limited to criticality calculations [7].

MAKXSF

MAKXSF is a utility program for manipulating cross section library files for use in MNCP5. The basic functions performed by MAKXSF include: changing the format of cross section libraries, copying entire libraries to new files or to copy selected nuclide data sets to new libraries, and to create nuclide datasets at new temperatures, resulting in a temperature dependent library for specific application [8].

Capabilities of MAKXSF for creating nuclide datasets at a new temperature involves three operations: 1) Doppler broadening of resolved data to any higher temperature, 2) Interpolation of unresolved resonance data between datasets at two different temperatures, and 3) Interpolation of thermal scattering kernels ($S(\alpha,\beta)$ data) between datasets at two different temperatures.

2.1.2 SCALE

The Standardized Computer Analysis for Licensing Evaluation (SCALE) code system serves in conjunction with MCNP to provide code-to-code benchmarking when applicable and for additional analysis beyond that of MNCP. SCALE is developed and maintained by Oak Ridge National Laboratory (ORNL) and is widely accepted around the world for criticality safety analysis, radiation source term and shielding, problem dependent resonance self-shielding of cross section data, sensitivity and uncertainty, and reactor physics analysis [9].

KENO-VI

KENO-VI is a functional module in the SCALE system. It is a mutigroup Monte Carlo code applied to determine the effective multiplication factor (k_{eff}) for three-dimensional systems. The geometry package in KENO-VI is capable of modeling any volume that can be constructed using quadratic equations [10].

ORIGEN-S

ORIGEN-S is a depletion and decay module in the SCALE code system, and it can be called from a control module or run as a stand-alone program. ORIGEN-S computes time-dependent concentrations and radiation source terms which are simultaneously generated or depleted through neutronic transmutation, fission, and radioactive decay [11]. In relation to this report,

ORIGEN-S was used in stand-alone mode for calculating spent fuel radiotoxicities and decay heat terms as a function of time for the TRU nuclides and fission products.

2.1.3 NFCSS

This code package was utilized to provide a code comparison for the front-end component models, and is not part of the final fuel cycle simulation tool platform. The International Atomic Energy Agency's (IAEA) simulation system, Nuclear Fuel Cycle Simulation System (NFCSS) was used to model fuel cycle components. NFCSS is a scenario based computer model for the estimation of nuclear fuel cycle material and service requirements. It has been designed to quickly estimate long-term fuel cycle requirements and actinide production. Natural uranium, conversion, enrichment, and fuel fabrication quantities are predicted. Additionally, the quantities and qualities (isotopic composition) of unloaded fuels are evaluated.

The IAEA developed CAIN (CAlculation of Inventory of spent fuel) specifically for the needs of NFCSS. CAIN solves the Bateman's Equations for a point assembly using one group neutron cross sections. In order to meet the accuracy, simplicity, and speed requirements a set of assumptions were built into the code. CAIN currently has 28 reaction and decay chains during irradiation and 14 decay chains during cooling [12].

2.1.4 MATLAB/Simulink

MATrix LABoratory (MATLAB) first appeared in the late 1970s and was originally designed to simplify the implementation of numerical linear algebra routines [13]. MATLAB has since grown into something much bigger, and it is continually developed by the MathWorks Corporation. It is both a powerful computational environment and a programming language that easily handles matrix and complex arithmetic. Typical uses include math/computation, algorithm development, modeling, simulation/prototyping, data analysis, exploration, visualization, scientific graphics, and application development.

Simulink works with MATLAB to offer modeling, simulation, and analysis of multidomain dynamic systems under a graphical user interface environment. Simulink includes a comprehensive set of customizable block libraries for both linear and nonlinear analyses. As Simulink is an integral part of MATLAB, it is easy to switch back and forth during analysis making it possible to take advantage of the features offered in each environment. The available options and flexibility of MATLAB/Simulink make it an ideal candidate for developing an integrated system model.

The numerical computing environment and programming language MATLAB serves as the shell, or driver, for the simulated nuclear energy system by interfacing the configuration of nuclear reactors and corresponding fuel cycle components. Simulink, an extension of MATLAB, is utilized for storing system output results and parameters, tracking material streams, data processing, and predicting system performance.

3 REACTOR AND FUEL CYCLE COMPONENT MODELS

The evaluated fuel cycle options are composed of different reactors and components that work in coordination with each other to produce the desired output. Each has its own function and each is considered in a standalone fashion. When possible experiment-to-code and code-to-code benchmarking procedures were applied with results presented within.

3.1 Nuclear Reactors

The performance of the fuel cycle is heavily based on the reactor units. The three reactors evaluated are the AP1000, VHTR, and ABR. The AP1000 is a Gen-III+ PWR design by Westinghouse. The VHTR is a Gen-IV design and currently the candidate for the Next Generation Nuclear Plant (NGNP). It is the prismatic core design and utilizes the Tri-structural isotropic (TRISO) fuel type. The ABR is a fast neutron spectrum system that is designed to burn actinides and eliminate waste.

3.1.1 AP1000

The AP1000 is a Westinghouse Electric Company reactor design and is the first Generation III+ reactor to receive final design approval from the NRC. The AP1000 is a two-loop PWR planned to produce 1154 MW_e. The design is built on proven technology from over 35 years of PWR operating experience. Major improvements over Gen-III reactors include the utilization of passive safety technology, overall system simplification, and modular construction. These improvements make the AP1000 safer, easier and less expensive to build, operate, and maintain.

The major design parameters for the AP1000 are similar to that of other PWRs. The thermal power is rated at 3400 MW_{th} and with a thermodynamic efficiency of 32.8%, it can produce a usable electrical power of 1115 MW_e. The fuel type is enriched UO_2 and the coolant/moderator is light water. A listing of the AP1000 design parameters are provided in Table 3.1.

Table 3.1. AP1000 Design Parameters.

Thermal power (MW_{th})	3400
Electrical power (MW_e)	1115
Thermodynamic efficiency (%)	32.8
Fuel	UO_2
Average fuel enrichment (wt %)	3.8
Type of fuel assembly	17x17
Number of fuel assemblies	157
Active fuel length (m)	4.3
Equivalent core diameter (m)	3.04
Operating cycle length (months)	18
Linear heat rating (kW/m)	18.7
Operating pressure (Mpa)	15.5
Coolant	Light Water
Coolant inlet temperature (°C)	280.7
Coolant outlet temperature (°C)	321.1

Model Description

MCNP and SCALE were used for modeling the AP1000. The reactor core consists of 157 fuel assemblies that are arranged to form a right circular cylinder. Each fuel assembly contains 264 fuel rods, 24 guide tubes for control rod clusters, and one centrally located guide tube for in-core instrumentation, all of which are arranged in a 17 x 17 square lattice array. Figure 3.1 shows a cross-sectional view of the fuel assembly and related fuel rod and guide tube placements.

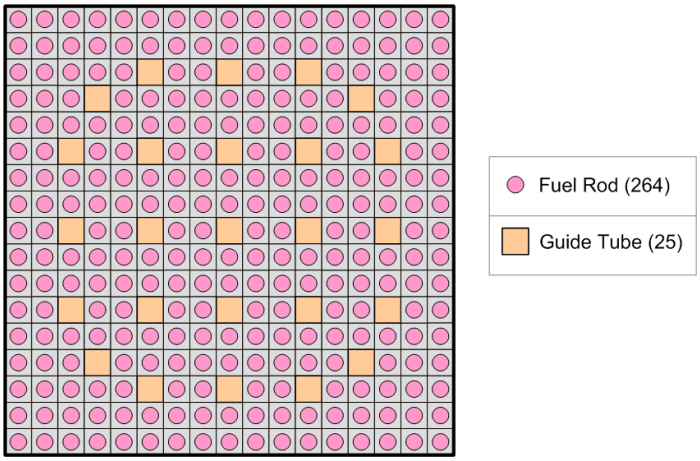

Figure 3.1. AP1000 Fuel Assembly.

The model design is based on the initial core loading, in which the fuel rods within any given assembly have the same uranium enrichment in both the radial and axial planes. Fuel assemblies of three different enrichments are used to establish a favorable radial power distribution.

Figure 3.2 shows the fuel assembly loading pattern used for the AP1000 model. It also shows the placement of the assemblies containing the Discrete Burnable Absorber (PYREX) rods and Integral Fuel Burnable Absorber (IFBA) rods within the core.

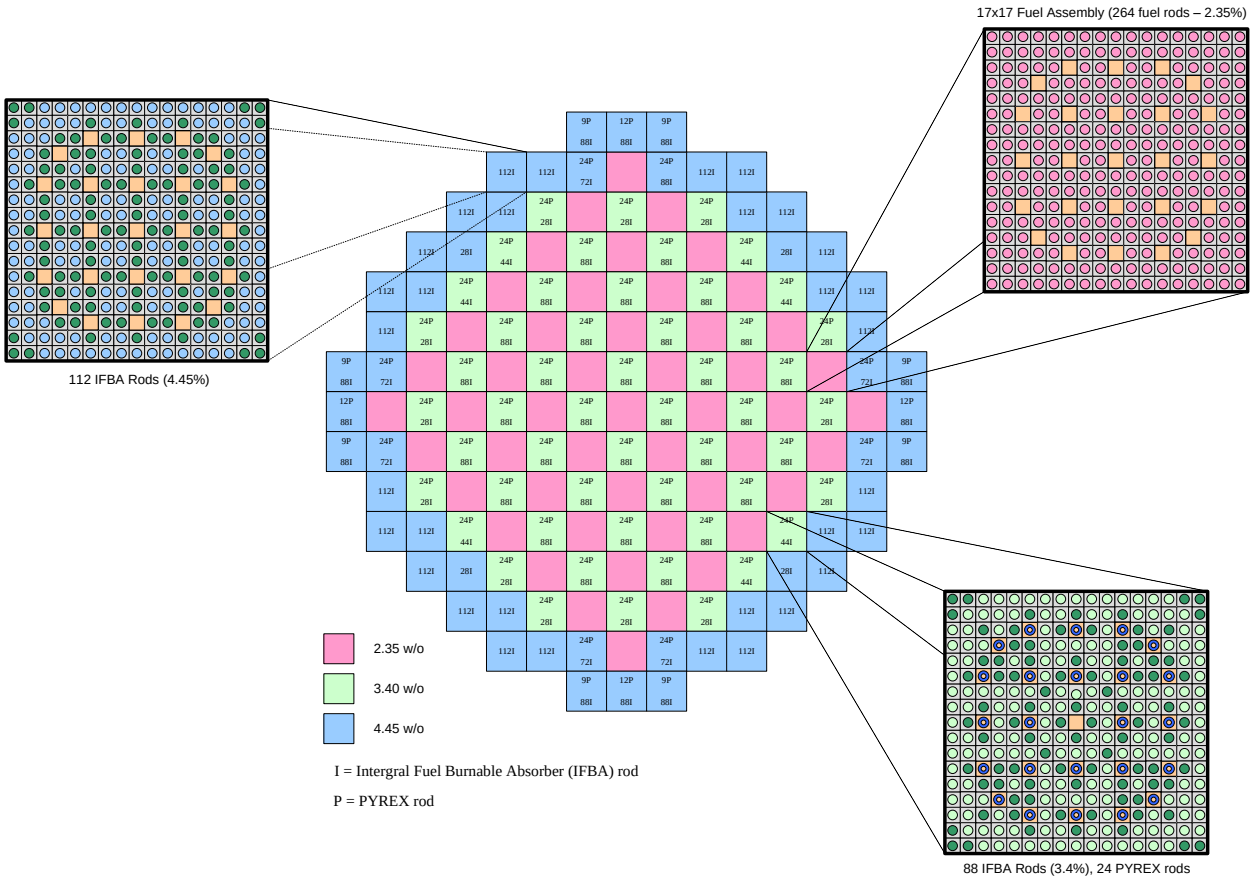

Figure 3.2. AP1000 Reactor Core Map.

Burnable absorbers in the form of PYREX and IFBA rods are used to provide partial control of the excess reactivity present during the fuel cycle. Their main function is to limit peaking factors and prevent the moderator temperature coefficient from being positive at normal operating conditions. Within a chosen fuel assembly, the PYREX rods can be arranged in one of three different configurations, as shown in Figure 3.3. Similarly, the IFBA rods can be arranged in five different configurations as shown in Figure 3.4. The placement of the assemblies containing the burnable absorber within the core is displayed in Figure 3.2. A description of the reactor core, including dimensions and core materials, is provided in Table 3.2.

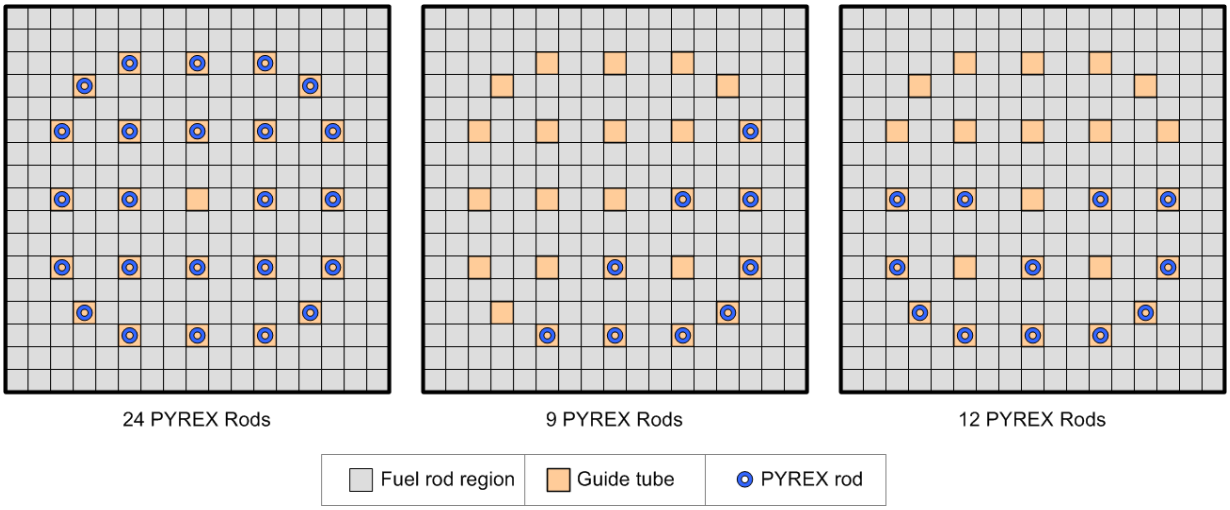

Figure 3.3. PYREX Rod Arrangement within the AP1000 Fuel Assembly.

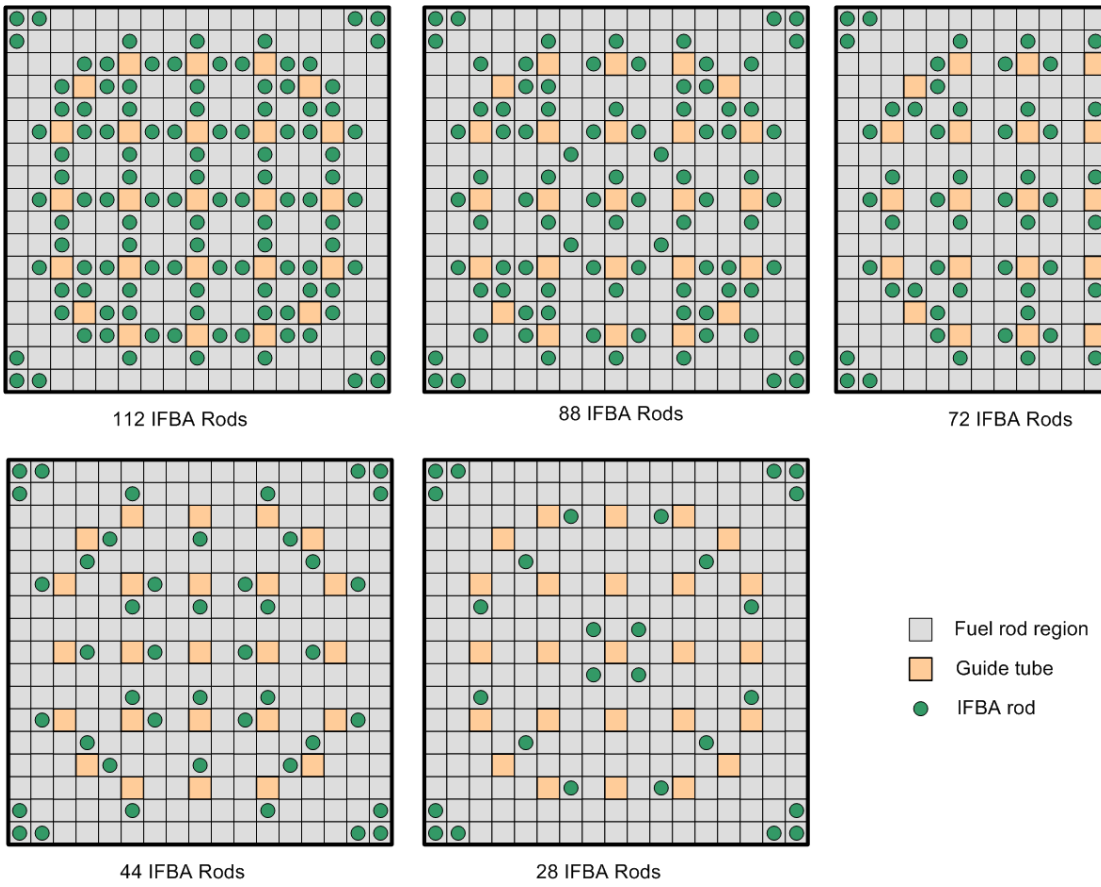

Figure 3.4. IFBA Rod Arrangement within the AP1000 Fuel Assembly.

Table 3.2. AP1000 Reactor Core Description.

Active Core	
Equivalent diameter (cm)	304.04
Active fuel height (cm)	426.72
Height-to-diameter ration	78.14
Total cross section area (m^2)	7.26
Fuel weight, as UO_2 (g)	9.76×10^7
Fuel Assembly	
Number	157
Rod array	17x17
Rods per assembly	264
Rod pitch (cm)	1.26
Overall transverse dimensions (cm)	21.40
Fuel Rods	
Number	41448
Outside diameter (cm)	0.9500
Gap diameter (cm)	0.0165
Clad thickness (cm)	0.0572
Clad material	ZIRLO
Fuel Pellets	
Material	UO_2 sintered
Density (% theoretical)	95.5
Fuel Enrichments (weight percent)	
Region 1	2.35
Region 2	3.40
Region 3	4.45
Diameter (cm)	0.819
Length (cm)	0.983
Discrete Burnable Absorber Rods (PYREX)	
Number	1558
Material	Borosilicate Glass
Outside diameter (cm)	0.968
Inner diameter (cm)	0.461
Clad material	Stainless Steel
B_{10} content (Mg/cm)	6.24
Absorber length (cm)	368.30
Integral Fuel Burnable Absorbers (IFBA)	
Number	8832
Type	IFBA
Material	Boride Coating
B_{10} content (Mg/cm)	0.772
Absorber length (cm)	386.08
Absorber coating thickness (cm)	0.00256

Benchmark Analysis

To test the validity of the AP1000 whole-core 3D model, a benchmark test was developed. The AP1000 Design Control Documentation [14] provided by the US NRC for the licensing process was used for the procedure. The report provided the multiplication factor (k_{eff}) for cold, zero power, beginning of cycle, and zero soluble boron core conditions. The code systems, MCNP5 and KENO-VI, were used to model the reactor at the specified core conditions in order to benchmark the k_{eff} value against published results and for a code-to-code benchmark procedure.

The results are listed in Table 3.3. As indicated, the MCNP calculation was very accurate when compared to the published results, giving a difference of only 0.0498% between k_{eff} values. The result calculated by SCALE had a slightly higher difference at 0.1942%. Comparing the two codes systems (MCNP vs. SCALE) the difference was measured at 0.1445%.

Table 3.3. AP1000 Multiplication Factor Results.

Multiplication Factor Origin	k_{eff}	% difference (published-to-code)	% difference (code-to-code)
AP1000 Design Control Documentation	1.2050	na	na
MCNP Code System (version 5 1.51)	1.2044	0.0498	0.1445
SCALE Code System (KENO-VI)	1.2026	0.1942	

The average energy-dependent neutron flux in the fuel elements, as produced by MCNP and SCALE, are provided in Figure 3.5. As shown, the thermal flux profile is as expected for a PWR. The spectrum produced by MCNP and SCALE are nearly identical.

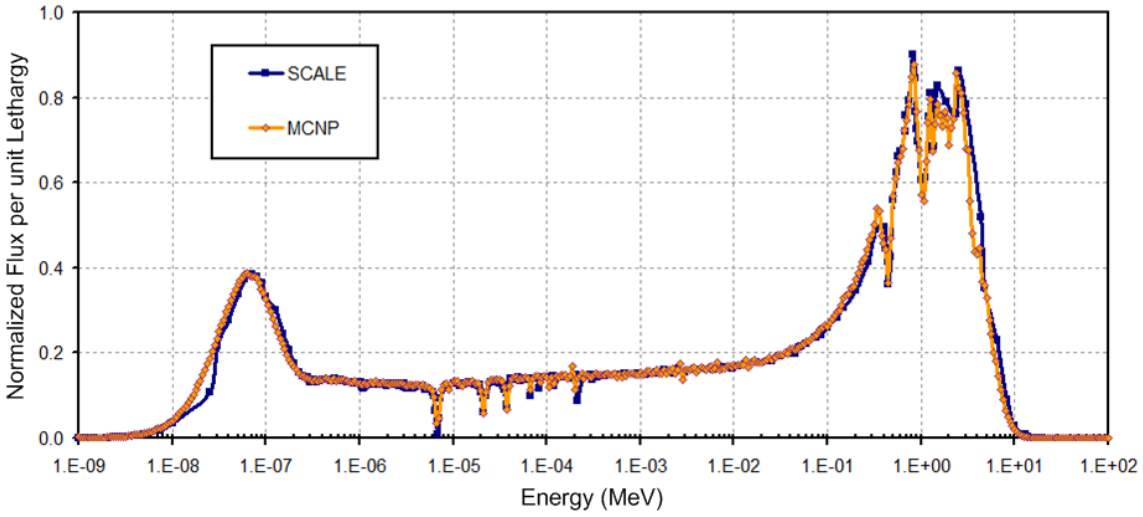

Figure 3.5. Neutron Flux Profiles in the AP1000 Fuel Rods (MCNP vs. SCALE).

3.1.2 VHTR

The VHTR is designed to be a high-efficiency system, which can supply electricity and process heat to a wide-range of high temperature and energy intensive applications. The VHTR is a passively safe design. The refractory core, low power density, and low excess reactivity enable this design feature.

The VHTR is a graphite moderated gas-cooled reactor that supplies heat with core outlet temperatures in the range of 850 - 1000° C. This enables applications such as hydrogen production, process heat for the petrochemical industry, or seawater desalination. Its basic technology has been well established in former High Temperature Gas Reactors (HTGR), such as the German AVR and THTR prototypes, and the US Fort Saint Vrain and Peach Bottom prototypes. The VHTR extends the capabilities of HTGR to achieve further improvements in thermal efficiency and future additional high-temperature applications.

Model Description

The VHTR model was created using the MCNP and SCALE code packages and is based on the High Temperature Test Reactor (HTTR) of the Japan Atomic Energy Research Institute (JAERI) [15]. The HTTR was selected because of the documented experimental test results and the opportunity it presented for performing an experiment-to-code benchmark analysis. The basic design features of the smaller HTTR were used to create the scaled-up VHTR power reactor. The VHTR design parameters are listed in Table 3.4.

Table 3.4. VHTR Design Parameters.

Fuel	UO_2		Power (MW_{th})	*600*
Enrichment(%)	*8*		Power Density (W/cm^3)	*6.9*
Coolant	*He*		Pressure (MPa)	*7.0*
			Inlet/Outlet Temperature (°C)	*490/950*
# of Columns	*102*		# of Fuel Columns	*66*
			# of Control Columns	*36*
			# of Blocks/Column	*13*
Block Pitch (cm)	*36*		# of Fuel Pins/Fuel Block	*32*
Block Height (cm)	*58*		# of Burnable Poison Rods/Fuel Block	*2*
			Control Rods/Control Block	*2*
			Emergency Rods/Control Block	*1*
			Compact Pitch (cm)	*5.15*
			Fuel Hole Radius (cm)	*4.1*
			Compact Inner Radius (cm)	*0.5*
			Compact Outer Radius (cm)	*1.3*
Packing (%)	*30*		10.41 g/cm^3 Kernel Radius (cm)	*0.0300*
			1.14 g/cm^3 Buffer Radius (cm)	*0.0359*
			1.89 g/cm^3 PyC1 Radius (cm)	*0.0390*
			3.20 g/cm^3 SiC Radius (cm)	*0.0419*
			1.87 g/cm^3 PyC2 Radius (cm)	*0.0465*
			Matrix (g/cm^3)	*1.77*
			Block (g/cm^3)	*1.69*

Figure 3.6 shows the arrangement and dimensions of the prismatic fuel block. The measurements and material properties of the block are given in Table 3.5, with all measurements provided in units of cm.

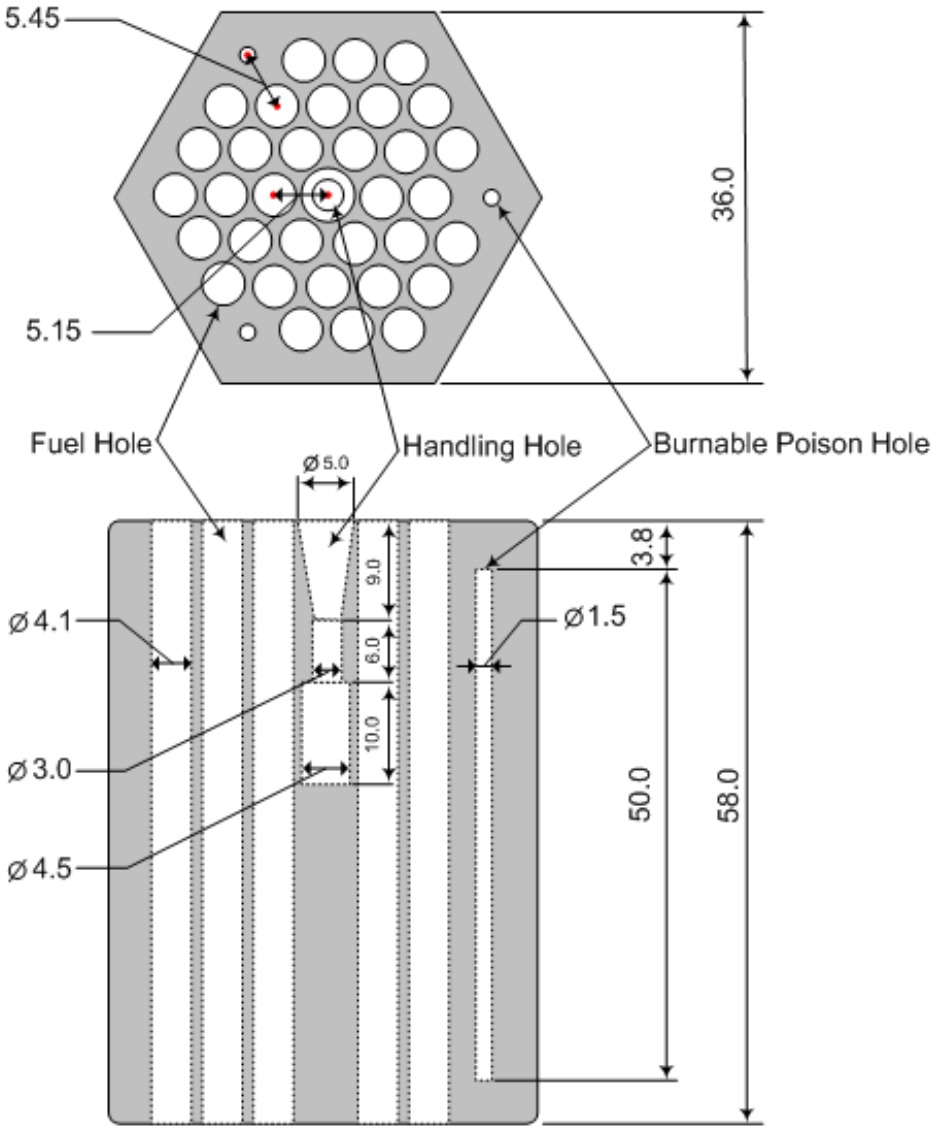

Figure 3.6. VHTR Prismatic Fuel Block (measurements in cm).

Table 3.5. VHTR Prismatic Fuel Block Properties.

Type	Pin-in-block
Configuration	Hexagonal
Material	IG-110 Graphite
Density (g/cm^3)	1.77
Height (cm)	58
Width Across the Flats (cm)	36
# of Fuel Holes/Block	33
Fuel Hole Diameter (cm)	4.1
Fuel Hole Height (cm)	58
# of Burnable Poison Holes/Block	3
Burnable Poison Hole Diameter (cm)	1.5
Burnable Poison Hole Height (cm)	50

The fuel element consists of TRISO fuel particles imbedded within a graphite matrix in the form of an annular rod (fuel compact), that is encapsulated by a graphite sleeve. Figure 3.7 illustrates how the TRISO particles, fuel compact, and protective sleeve are arranged to create the fuel element. Table 3.6 contains the fuel element dimensions and material properties.

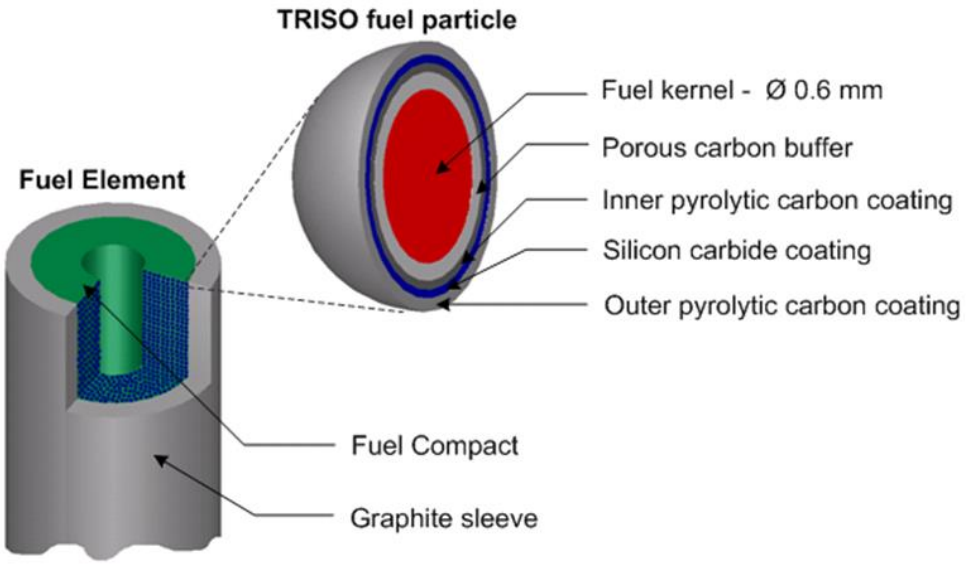

Figure 3.7. VHTR Fuel Element.

Table 3.6. VHTR Fuel Element Properties.

a) TRISO particle	Material	Density (g/cm³)	Radius (cm)
Fuel kernel	UO_2	10.41	0.0300
1st coating	PyC	1.14	0.0359
2nd coating	PyC	1.89	0.0390
3rd coating	SiC	3.2	0.0419
4th coating	PyC	1.87	0.0465

b) Fuel Compact		c) Graphite Sleeve	
Number of fuel particles	176,515	Material	Graphite
Graphite matrix density	1.690 g/cm³	Density	1.770 g/cm³
Diameter-inner	1.0 cm	Diameter-inner	2.6 cm
Diameter-outer	2.6 cm	Diameter-outer	3.4 cm
Height	54.6 cm	Height	57.7 cm

Figure 3.8 shows a three-dimensional representation of the prismatic fuel block and the relative locations of the annular fuel rods, coolant channels, burnable poison rods, and fuel-handling hole.

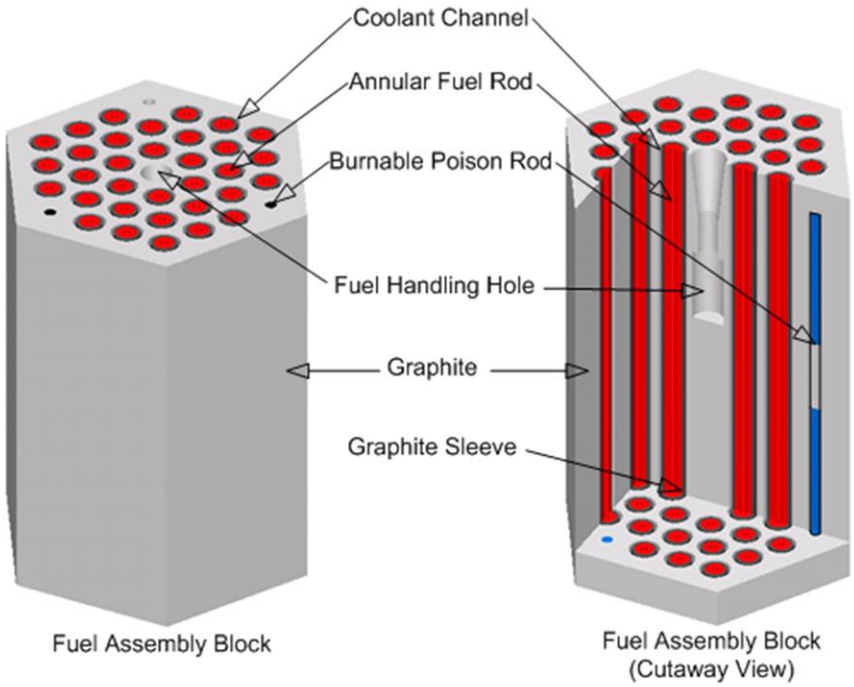

Figure 3.8. VHTR Prismatic Fuel Block.

The active core is composed of 858 fuel columns arranged in an annular configuration with a central and surrounding graphite reflector. The active core is 754 cm in height and the overall core is 1030 cm in height. The radial distance from the center of the core to the closest fuel

column is 144 cm and the fueled region is 108 cm thick (three fuel/control columns across). The outer reflector is 88 cm thick giving an outer cylindrical core radius of 340 cm. Figure 3.9 shows a 3D and 2D view of the VHTR model with geometry details.

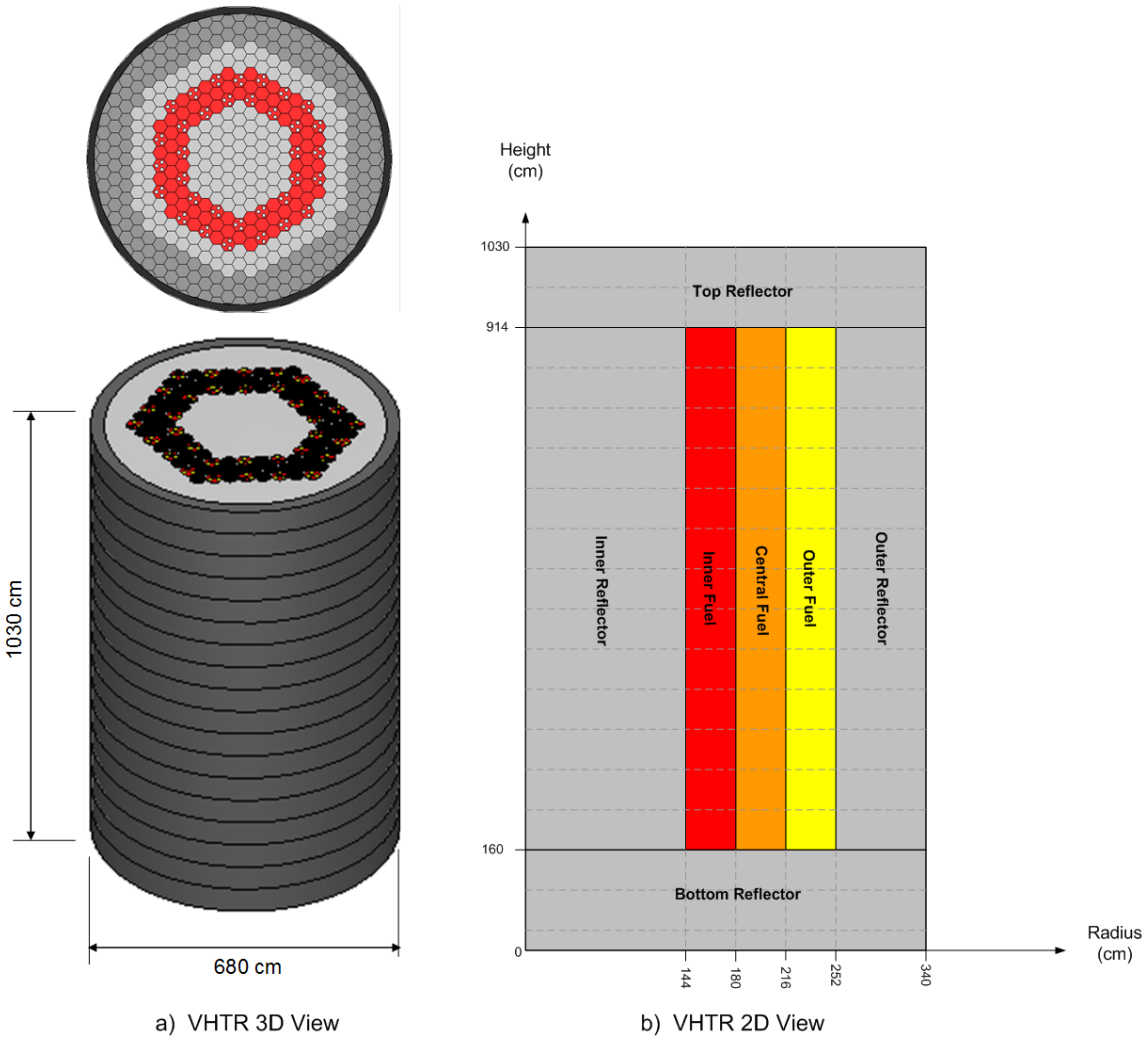

Figure 3.9. VHTR Model Geometry Details.

Benchmark Analysis

Importance was placed on the ability to perform experiment-to-code benchmarking and to combine that with additional code-to-code comparisons. The availability of experimental results led to the HTTR of the JAERI, from which startup core physics results are provided by the IAEA in a Technical Document publication [15]. A complete set of details for the benchmark analysis are included in Appendix A.

The benchmark problems are related to start-up core physics tests and include the analysis of the effective multiplication factor for the fully loaded core with control rods fully withdrawn and fully inserted, control rod position at criticality, and the isothermal temperature coefficient of reactivity. Table 3.7 shows the results for the benchmark analysis.

Table 3.7. Benchmark Results.

Benchmark		HTTR (experimental)	VHTR model (calculated)	Error (%)
Control Rods Fully Withdrawn	k_{eff}	1.1363 ± 0.041	1.1368 ± 0.0023	0.044
Control Rods Fully Inserted	k_{eff}	0.685 ± 0.010	0.6858 ± 0.0019	0.117
Critical Insertion Depth (300K)	cm	177.5 ± 0.5	177.1	0.225
Critical Insertion Depth (418K)	cm	190.3 ± 0.5	189.9	0.210
Temperature Coefficient	Δk/k/K	-1.42×10^{-4}	-1.45×10^{-4}	2.113

The whole-core model was adjusted from the original cylindrical core of the HTTR to that of a larger annular power core. To maintain consistency an exact model was built in SCALE and MCNP to perform a code-to-code benchmark for the new configuration. A comparison of the multiplication factor for each is provided in Table 3.8.

Table 3.8. VHTR Code-to-code Results.

Code System	k_{eff}	% difference
MCNP5	1.26737	0.124
SCALE (KENO-VI)	1.26580	

The average energy-dependent neutron flux within the fuel compacts was evaluated for the models. Figure 3.10 shows that the profile for MCNP and SCALE are in agreement and typical for that of VHTRs.

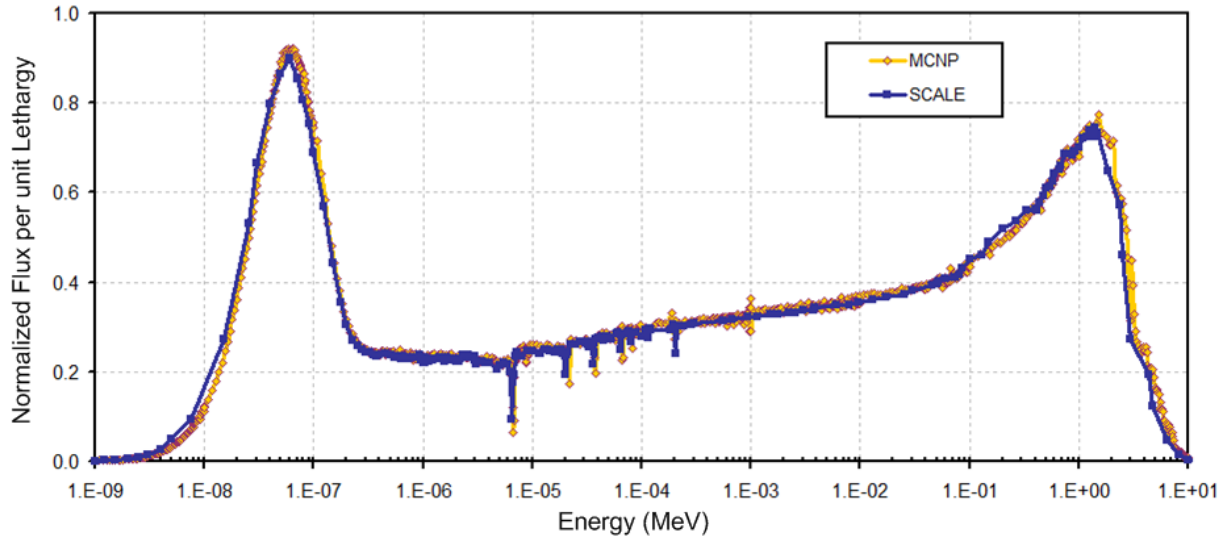

Figure 3.10. Neutron Flux Profiles in the VHTR Fuel Compacts.

3.1.3 ABR

The ABR is based on the SuperPRISM (S-PRISM) 1000 MW_{th} [16] reactor, which is a pool-type sodium-cooled fast reactor designed to operate as a breeder or near breakeven. The Argonne National Laboratory (ANL) report ANL-AFCI-177 [17] provided the reference source for the ABR. The core is intended to transmute recycled TRU elements and thus operates at a reduced conversion ratio, as compared to the S-PRISM. The design uses U-TRU-Zr alloy metal fuel, operates without blankets, and has a conversion ratio of 0.05.

Model Description

MCNP and SCALE were used for whole-core 3D models of the core. The fuel pin and assembly dimensions are provided in Table 3.9 The fuel pins include sodium bond between the fuel and cladding and a gas plenum. Figure 3.11 provides visual representation of the 324 pins per assembly

Table 3.9. ABR Fuel Pin and Assembly Design.

Fuel Pin	
Fuel radius (cm)	0.2415
Clad radius (cm)	0.3115
Pitch (cm)	0.80554
Fuel smear denisty (%)	75
Fuel height (cm)	101.06
Plenum heigth (cm)	191.14

Fuel Assembly	
Hexagonal Assembly Pitch	16.142
Fuel Pins	324
Empty Cells (Na)	7
Duct width across flats (cm)	15.71
Duct thickness (cm)	0.394
Duct material	HT9

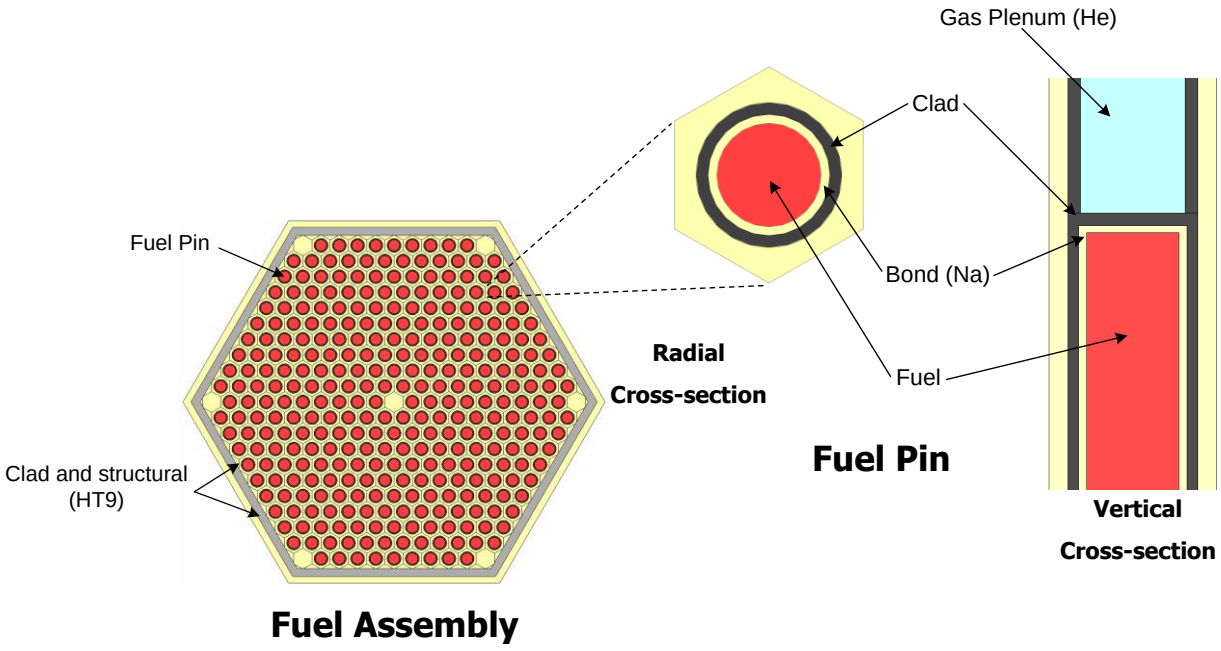

Figure 3.11. ABR Fuel Assembly and Fuel Pin.

The core consists of 144 driver fuel assemblies that are divided into inner, middle, and outer fuel regions, as shown in Figure 3.12. The regions differ by TRU enrichment allowing for flattening of the power distribution. The three outer rings of the core are made up of the reflector and shield. The control elements were modeled as fully withdrawn.

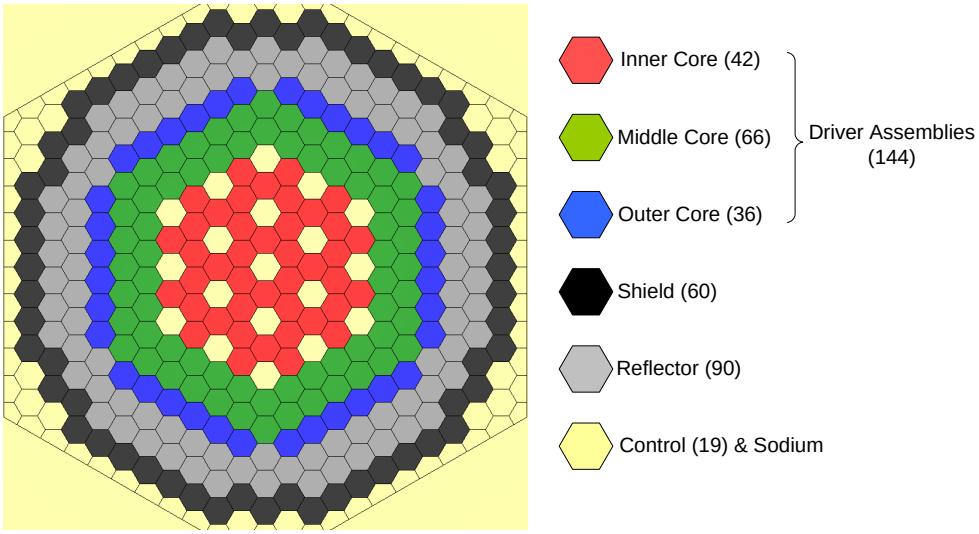

Figure 3.12. ABR Core Layout.

The TRU fuel composition was taken from the ANL-AFCI-177 report and is listed in Table 3.10. The composition is representative of PWR fuel irradiated to 50 GWd/MT and include discharge and reprocessing times.

Table 3.10. ABR Fuel Composition.

Fuel (Density = 15.1 g/cc)			
	Inner core	Middle core	Outer core
U, w/o	66.1	58.7	51.7
TRU, w/o	23.9	29.3	34.3
Zr, w/o	10	12	14
isotope	w/o	w/o	w/o
Zr	10	12	14
U-235	0.1322	0.1174	0.1034
U-238	65.9678	58.5826	51.5966
Np-237	1.141703	1.399661	1.638511
Pu-238	0.55209	0.67683	0.79233
Pu-239	11.447861	14.034407	16.429357
Pu-240	5.37989	6.59543	7.72093
Pu-241	2.52862	3.09994	3.62894
Pu-242	1.558041	1.910067	2.236017
Am-241	0.802084	0.983308	1.151108
Am-242m	0.001434	0.001758	0.002058
Am-243	0.352525	0.432175	0.505925
Cm-243	0.001195	0.001465	0.001715
Cm-244	0.123085	0.150895	0.176645
Cm-245	0.009799	0.012013	0.014063
Cm-246	0.001195	0.001465	0.001715

Comparison Between Independent Models

The multiplication factors predicted by MCNP at different time steps were compared to those calculated by a study performed at Idaho National Laboratory [18] using the code packages MC^2-2 and REBUS. The results for this comparison are listed in Table 3.11. As indicated, MCNP over predicted k_{eff} and although refinements could be made to approach better agreement, for the purposes of this study the ABR model was considered appropriate

Table 3.11. Multiplication Factor Comparison.

Time (days)	INL model	MCNP	% difference
0	1.0288	1.0442	1.47
54	1.0217	1.0384	1.61
108	1.0146	1.0301	1.50
163	1.0075	1.0203	1.25
217	1.0006	1.0098	0.91

3.2 Fuel Cycle Components

3.2.1 Front-end Components

The front-end portion of the cycle includes mining, milling, conversion, enrichment, and fuel fabrication. As a result of front-end procedures, DU and mill tailings are accumulated and must be stored as LLW. The main concern for the front-end is material flow and its effect on mining and waste storage strategies.

The front-end components are modeled in the Simulink/MATLAB environment. The model tracks the overall material flow in each of the processes shown in Figure 3.13. The model assumes zero losses in the conversion, enrichment, and fuel fabrication stages.

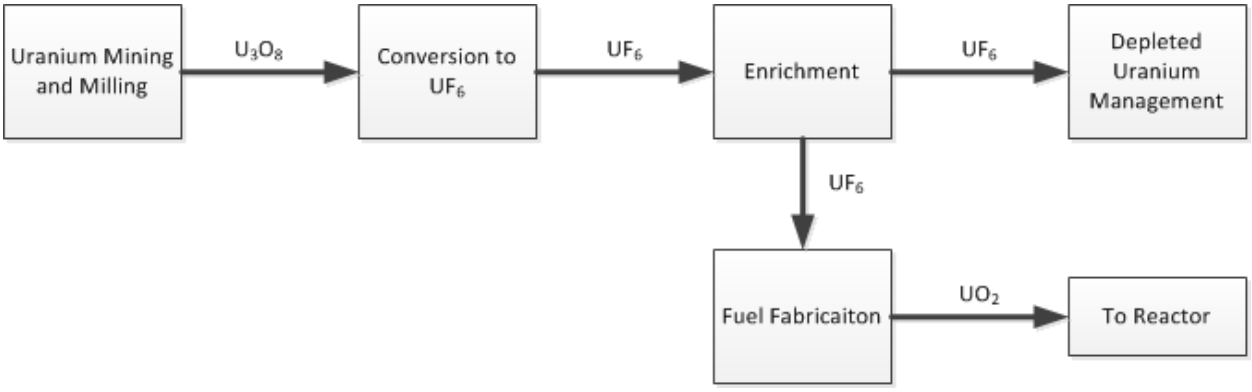

Figure 3.13. Front-end Model Components.

A mass balance relating the throughput for each process to the electricity produced by the AP1000 is used to back propagate material quantities, as indicated by:

$$E\left[\frac{GJ}{MWh(e)}\right] = f\left(BU, \eta, x_p, f_u\right),$$

where BU is the fuel burnup, η is the thermal efficiency, f_u is the ratio of the mass of enriched product (M_p) to the mass of the feed material (M_f), and x_p is the weight percent enrichment in U^{235}.

The values for BU, η, M_f , and x_p are feed into the calculation from the AP1000 model. In order to determine f_u an additional calculation is needed:

$$M_f = M_p \frac{x_p - x_w}{x_f - x_w},$$

where x_w is the weight fraction of U^{235} in the waste stream and x_f is the weight fraction of U^{235} in the feed material.

The Seperative Work Unit (SWU) for the enrichment process is determined by the following relationships:

$$SWU = M_p V_p + M_w V_w - M_f V_f$$

$$V\left(x_i\right) = \left(1 - 2x_i\right)\ln\left(\frac{1 - x_i}{x_i}\right)$$

where x_i stands for x_f, x_p, x_w, and V is the separation potential.

Environmental impact measures (energy requirements, CO_2 emissions, water requirements, and land use) for the front-end components are also calculated. Operational data for operating facilities, projections taken from facility engineering design studies, and conceptual design level studies are used to obtain curve fit parameters and determine coefficients in order to estimate the environmental footprint. The procedure followed that as outlined by INL report INL/EXT-10-20652 [19].

The input and output variables for the front-end model are listed in Tables 3.12 and 3.13.

Table 3.12. Front-end Input Variables.

Parameter	Range/Option
AP1000 fuel enrichment	3 - 8 %
AP1000 fuel burnup	30 - 90 GWd/MT
AP1000 capacity factor	80 - 100 %
Uranium ore grade	0.01 - 19 %
Mining stripping ratio	0 - 40
Enrichment technology	diffusion, centrifuge (individual or combination)
Mining technology	open pit, underground, in-situ leaching (individual or combination)
Fuel fabrication type	UOX, MOX

Table 3.13. Front-end Computational Output.

Material quantities (kg U)
Depleted Uranium (composition, kg)
Seperative Work Units (kg)
Component Energy consumption (GJ/MWh)
Component carbon footprint (kg CO_2/MWh)
Component Water requirements (L/MWh)
Component Land usage (m^2/MWh)

3.2.2 Reprocessing - Partitioning/Separation

The computational model representing the reprocessing process was designed to track the material streams while accounting for radioactive decay and material losses accrued during the procedure. The material tracks are modeled according to the URanium Extraction (UREX) process in which the Uranium and Technetium are separated from each other and the other FP and actinides. A suite of UREX+ processes offer the ability to produce different product lines with varying mixtures of actinides and FPS. The process used for the modeling purposes is UREX+1a, which has five product lines made up of: 1) Uranium, 2) Technetium, 3) Cesium/Strontium, 4) TRU, and 5) remaining FP. In addition to tracking materials, the model creates a database for storing material compositions for varying AP1000 and ABR input parameters making them easily assessable for analysis. The numerical computational environment MATLAB is utilized for the simulation procedure and material database storage.

3.2.3 High Level Waste Storage Facility

The computational model for the waste storage facility applies normalized heat factors and normalized radiotoxicity factors for the TRU to quantify repository performance, which in turn can be used for making comparisons to other fuel cycles. It simulates a geological repository by tracking isotopic compositions over long periods of time and calculating resulting heat load and dose measurements in order to analyze waste management strategies. The ORIGEN-S code package is utilized for predicting radionuclide inventories after many years of decay. MATLAB is used for data processing involving dose and heat load calculations for assorted isotopic compositions.

3.3 Fuel Cycle System Model

The integrated system model was developed within the MATLAB/Simulink environment. Simulink works with MATLAB to offer modeling, simulation, and analysis of multidomain dynamic systems under a graphical user interface environment. Simulink includes a comprehensive set of customizable block libraries for both linear and nonlinear analyses. As Simulink is an integral part of MATLAB, it is easy to switch back and forth during analysis making it possible to take advantage of the features offered in each environment. The available options and flexibility of MATLAB/Simulink make it an ideal candidate for system modeling.

The main objective of the integrated model is to develop an approach to seamlessly couple the various models that compose the fuel cycle. The goal being to devise a computational shell that effectively controls the set of reactor and fuel cycle component models with command over key user input parameters and the ability to effectively consolidating vital output results into readily usable form, and to do so in a manner that allows uncertainty/sensitivity analysis and optimization procedures to be performed in a realistic and time efficient manner.

The computational model uses a specially prepared database to predict overall system performance and behavior based on a number of different input parameters that are allowed to vary over a specified range. The input parameters are introduced into a database and the appropriate data is retrieved and prepared to construct a function that describes the behavior of the data. An interpolation or extrapolation method is then called to calculate the corresponding data, which is then processed and manipulated into final output form, or fed back into the system to repeat the procedure as many times as necessary to obtain a set of output results corresponding to the input parameters. Figure 3.14 shows the basic operational procedures for the system model.

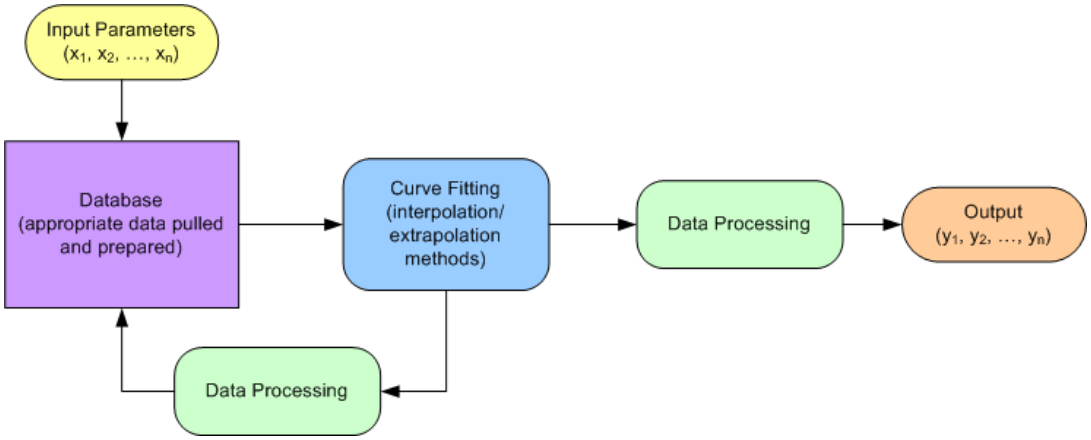

Figure 3.14. System Model Basic Flowchart.

The overall system is broken down into its individual components, which can be thought of as a set of interacting or interdependent entities (subsystems) forming an integrated whole. Each of the subsystems can also contain input variables, which, may or may not, progressively rely on one another as additional subsystems are added to the system.

The reactors and fuel cycle components represent the individual subsystems. The rational is that although the system model was developed with a particular fuel cycle option in mind, it can be modified to fit other systems that share common characteristics. For example, reactor components can be added or removed along with their related input variables, thus producing an entirely different advance nuclear fuel cycle option. A good candidate for simulation is any system that operates under similar characteristics and is composed of complicated subsystems that are extensively time consuming to model or study experimentally.

Changes made to system dependencies or to the dataflow in the system will be reflected in the database. The database structure and indexing is directly related to the subsystems, input variables, and their interdependence within the system.

Database

The database can be viewed as a set of multi-degree arrays that are arranged to allow quick computational access. The database is structured to match the number of subsystems and input variables within the system and the interdependence between them. With the database correctly populated and indexed, the system can efficiently map input to a set of output values by assembling a lookup table and then constructing the appropriate mathematical functions between selected data points and applying curve fitting techniques for interpolation or extrapolation methods.

The structure is arranged so that output information can be gathered for each input variable signifying the affect that that particular variable has at its specified level in the system. To accomplish this the database must include an individual data array for each of the input variables. The dimension of the array is incremental with the position of the variable in the overall system. Each array is a portion of the overall system's multi-dimensional array. This feature increases

the size of the database, but the uniqueness of the elements making up the database remain the same.

With the database populated and indexed accordingly, the system model calls the appropriate data for curve fitting and uses interpolation or extrapolation algorithms for calculating output data. Options for three methods are offered: rounding, linear, and cubic spline.

Data Processing

At all levels within the system the data can be processed and manipulated to fit the desired output form. Data processing is performed between each subsystem in order to maintain system compatibility. Output results can be processed and presented in many different forms giving the user latitude of selecting from many options. For example the data can be plotted, normalized, arranged in table or matrix format, compared to previous results, formatted for immediate use by other software analysis tools, stored for future use, etc. The available tools for processing data include, but are not limited to, the mathematical operations existing in the MATLAB/Simulink environment.

Figure 3.15 shows the data path and setup for the fuel cycle arrangement corresponding to FC2. It consists of five subsystems: front-end, AP1000, reprocessing, VHTR, and repository. The uranium and TRU path represent multiple isotopes, indicating that each has been collapsed to contain information that is applied similarly to the each of the isotopes they contain. The uranium path controls 4 isotopes, while the TRU path controls 15 isotopes.

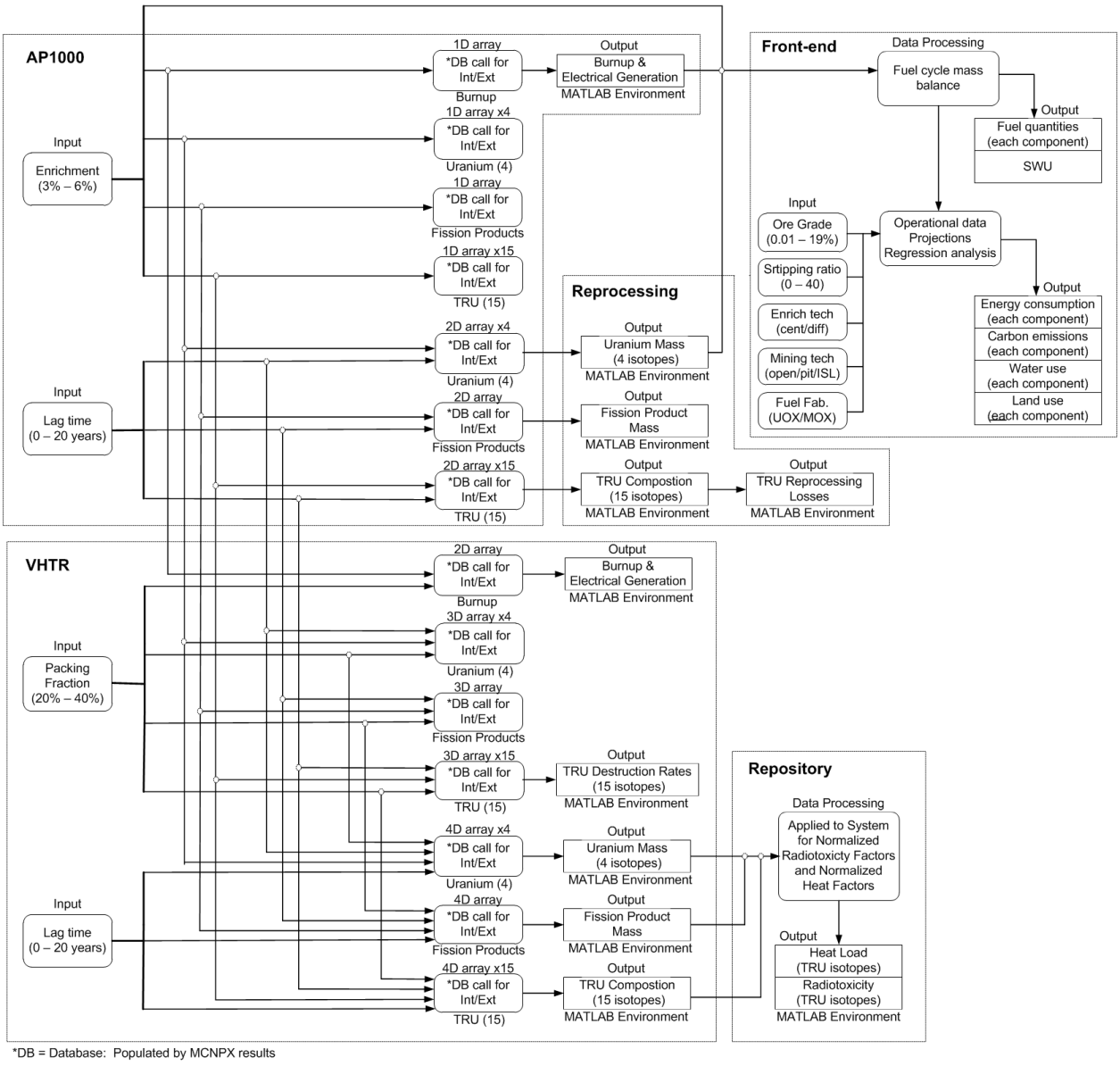

Figure 3.15. Dataflow Mapping for Fuel Cycle FC2.

The integrated model offers control and manipulation of the input parameters and the output can be modified countless different ways, since it is produced within the MATLAB environment. In addition, the computational cost of the simulation is minimal, especially when compared to MCNPX depletion calculations for the reactor systems.

4 NEUTRONIC AND FUEL CYCLE ANALYSIS

4.1 Front-end Components

The front-end components were modeled using the Simulink/MATLAB code package. Given the input parameters in Table 4.1 the fuel cycle mass balance can be performed. The results are given in Figure 4.1 and are normalized to produce 1 kg of uranium at 5% enrichment.

Table 4.1. Input Values for Mass Balance Calculation.

Burnup	57 GWd/tIHM
Thermal efficiency	32.80%
U235 enrichment in product	5.00%
U235 enrichment in feed	0.71%
U235 enrichment in waste stream	0.20%
Mass of enriched product	1 kg

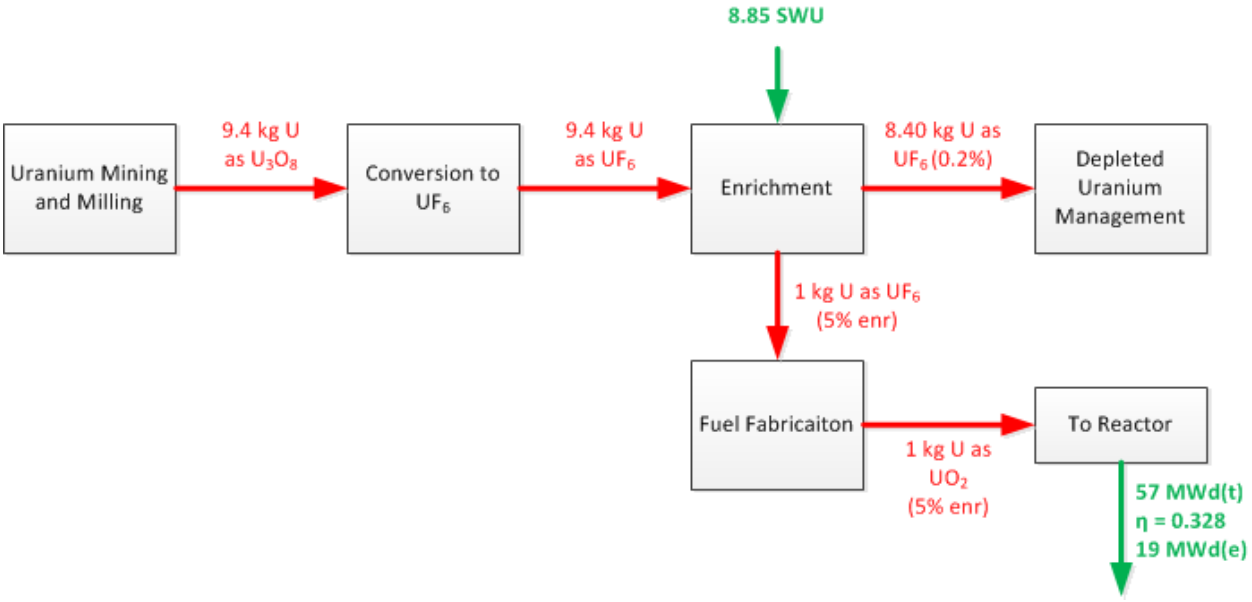

Figure 4.1. Mass Balance Results for Front-end Components.

Applying the input parameters from Table 4.1 above and considering a uranium ore grade of 0.1%, a stripping ratio of 4, a mining makeup (25% open pit, 40% underground, 35% ISL), centrifuge enrichment technology, and uranium oxide fuel fabrication, the following environmental impact measures are calculated, see Table 4.2.

Table 4.2. Environmental Impact Measures for Front-end Components.

	Energy Consumption GJ/MWh(e)	Carbon emissions kg CO_2/MWh(e)	Water use L/MWh(e)	Land use m^2/MWh(e)
Mining/milling	6.80E-03	0.79	126	7.35E-03
Conversion	2.58E-02	1.43	2.06	1.17E-05
Enrichment (centrifuge)	2.70E-03	0.42	0.66	1.31E-04
Fuel Fabrication (UOX)	6.24E-04	0.079	0.31	1.16E-05
DU Management (U_3O_8 shallow burial)	2.74E-04	0.032	0.22	1.80E-04
Totals	3.62E-02	2.751	129.25	7.68E-03

4.2 AP1000

As a first step AP1000 evaluations were performed for a reference core having an average fuel enrichment of 4.5 wt.% with a single batch fuel management scheme. The ENDF/B-VII cross-section library was used for fuel temperatures at 900K and moderator temperatures at 600K. Depletion calculations were performed by MCNPX using 50 day intervals and 700,000 neutron histories per interval.

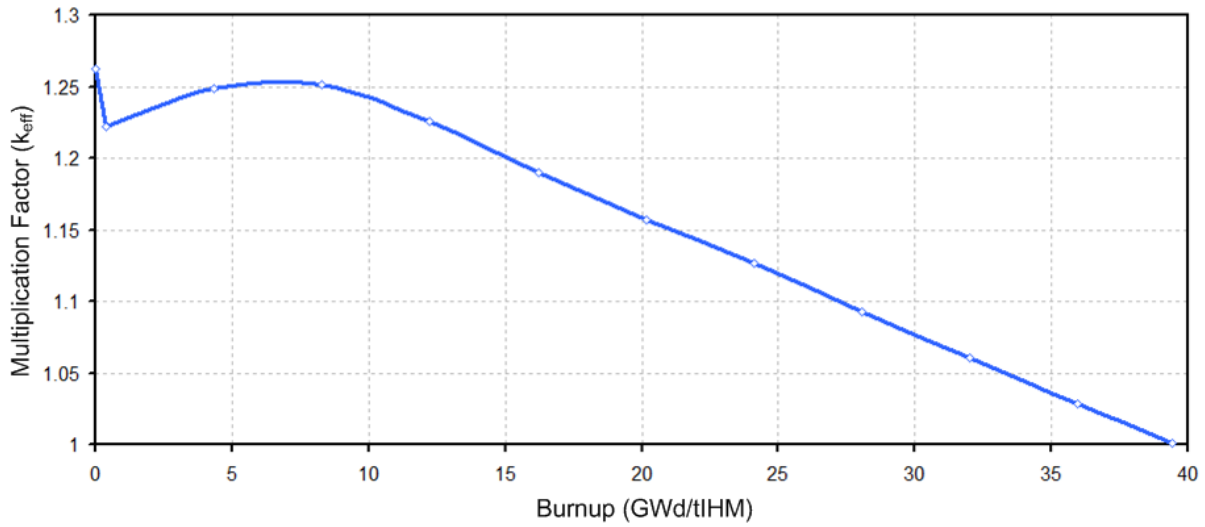

Figure 4.2. AP1000 Whole Core Depletion.

Figure 4.2 shows the time evolution of the AP1000 core k_{eff} determined by MCNPX. The core has an initial k_{eff} value of 1.26. A short time step was incorporated in the burnup scheme to show the neutron poison effect accompanying the introduction of FPs into the core at reactor startup. The reactivity level of the core then gradually increases for a short time period before decreasing again. The PYREX rods and IFBA rods that are present in the core cause the initial increase in k_{eff}. At Beginning of Cycle (BOC) the boron in the PYREX and IFBA rods acts as a strong neutron poison and significantly depresses the reactivity of the core, but as time progresses the boron is depleted, which is evident by the increase in k_{eff}. The core reaches a subcritical level at approximately 39.4 GWd/tIHM, which is equivalent to 997 Effective Full Power Days (EFPD).

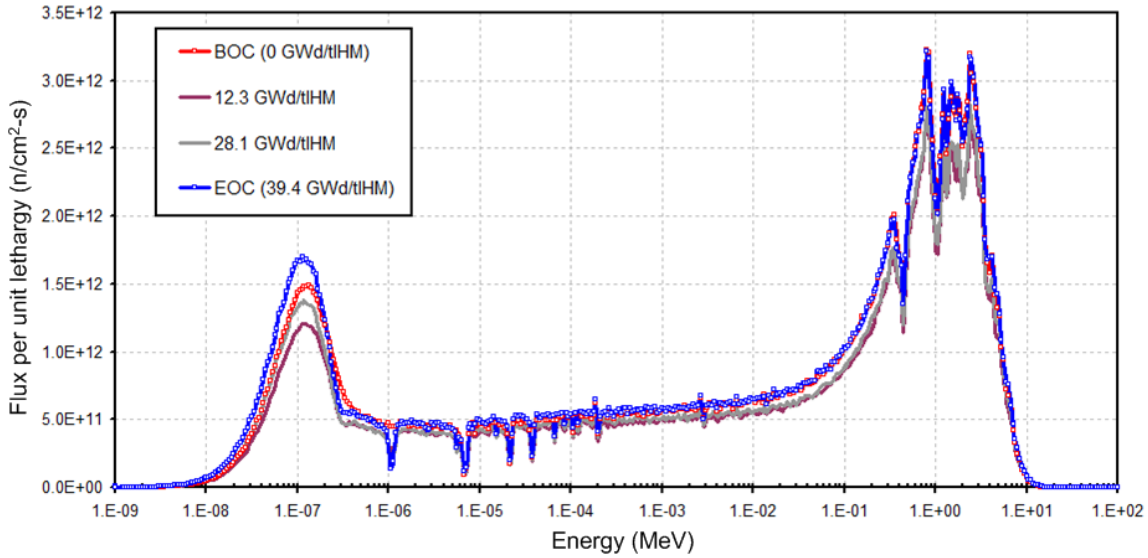

Figure 4.3. AP1000 Spectra at Different Burnup Levels.

The profile of the average neutron flux in the fuel elements at different burnup levels are provided in Figure 4.3. To maintain a constant power throughout the core lifetime, the flux must constantly change to compensate for the isotopic transformations caused by neutron irradiation. The main competing factors in the process are the consumption/production of fissile nuclides, the depletion of the burnable poisons, and the accumulation of fission products in the core. The spectrum profile in each case is similar with the most notable difference being the thermal energy peak. At BOC, the burnable poisons are at full strength, but as time evolves the powerful thermal energy neutron absorber ^{10}B is depleted and consequently less thermal energy neutrons are removed from the system. The depletion of Burnable Poison (BP) happens early in the core's lifetime and only a small fraction of the ^{10}B remains at a fuel burnup level of 15 GWd/ tIHM. The effect is evident by the decrease in the flux between BOC and 12.3 GWd/ tIHM. Additionally, as the burnup level increases the amount of total FP in the core continues to grow. The FP are neutron absorbers and over time have a strong negative effect on the core's neutron economy. Also, the fissionable material in the core is gradually decreased as ^{235}U is diminished throughout core lifetime and the production of ^{239}Pu and ^{241}Pu levels off towards the End of

cycle (EOC). The cumulative effect translates to an increase in neutron flux, as shown by the flux plots for burnup levels between 12.3 GWd/tIHM and EOC.

The evaluations above are useful for gaining insight into operational characteristics of the reactor core, but the AP1000 is planned to operate on a batch cycle. In order to simulate this affect the core was divided into zones and a three batch shuffling scheme was applied. The initial core matches the model used for benchmark analysis described in section 3.1.1, which has an average fuel enrichment of 3.8%. The startup core has three enrichment zones (2.35%, 3.40%, 4.45%), that are used to flatten the power profile. The first core shuffle removes zone 1 (core outer ring) from the reactor replacing it with the once burned fuel from zone 2 (core middle ring). The fuel in zone 1 (core center) is moved to zone 2, and fresh fuel is added to zone 1, as shown in Figure 4.4.

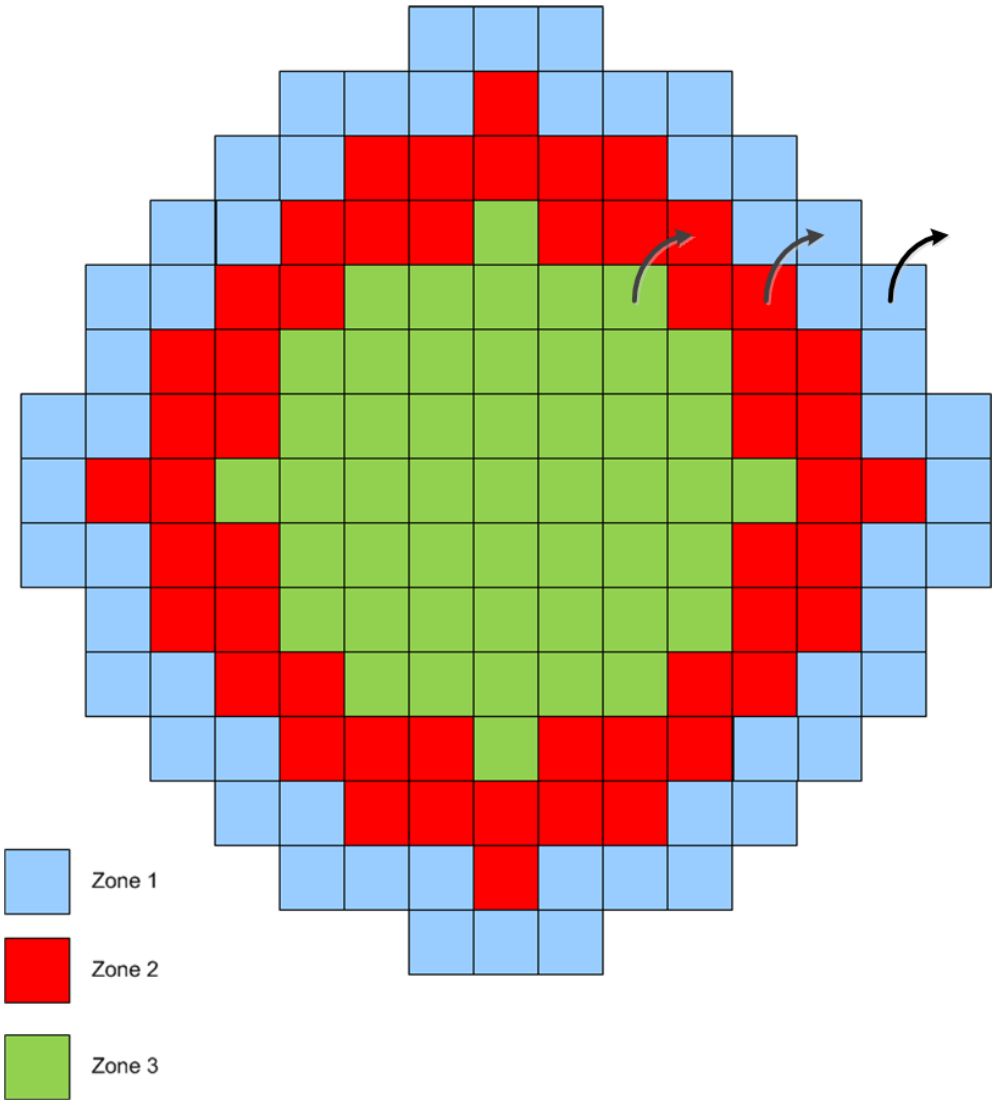

Figure 4.4. AP1000 Fuel Shuffling Scheme.

The shuffling scheme was applied for four cycles to reach an equilibrium core. Figure 4.5 shows the core multiplication factor as a function of time for fuel loading enrichments of 3%, 5%, and 8%. In each case a capacity factor of 100% was applied. The fuel burnup and duration vary from 33 - 89 GWd/tIHM, and 280 - 710 days. Table 4.3 list the defining characteristics for each enrichment case.

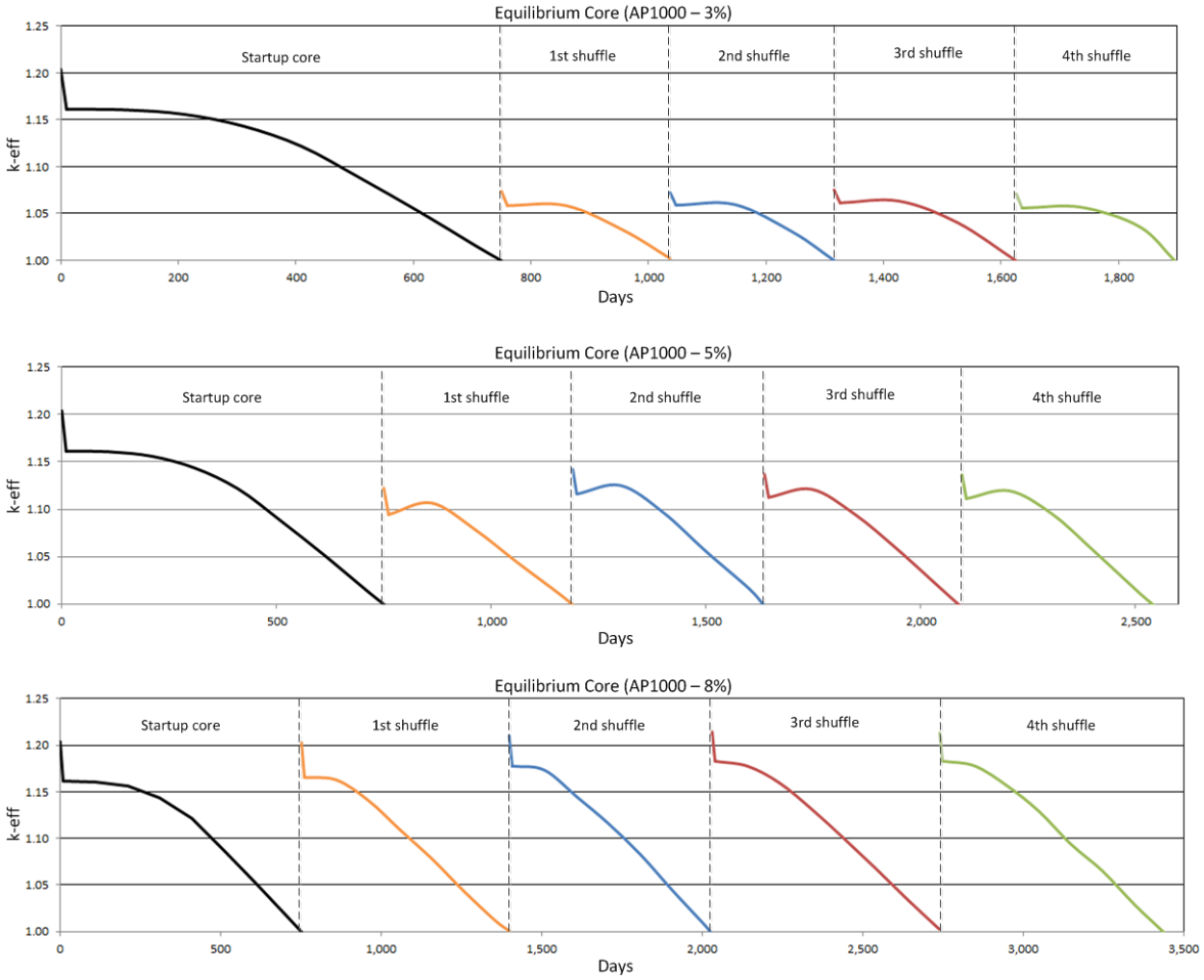

Figure 4.5. Depletion Sequence for AP1000 Equilibrium Core.

Table 4.3. Burnup and Batch Cycle Duration Results for AP1000 Equilibrium Core.

Enrichment (%)	Capacity Factor (%)	Batch Duration (days)	Burnup (GWd/tIHM)
3	100	280	33
5	100	450	57
8	100	710	89

The core is initially loaded with 86.1 MTU, with approximately 3.9 tones being ^{235}U. From the time of reactor startup the fissile component ^{235}U is depleted but other fissile components are produced when ^{238}U is transmuted to higher actinides, particularly ^{239}Pu and ^{241}Pu. Figure 4.6 shows the time evolution of important isotopes within the core, from which a comparison can be made between the consumption of the fuel and the production of important plutonium isotopes.

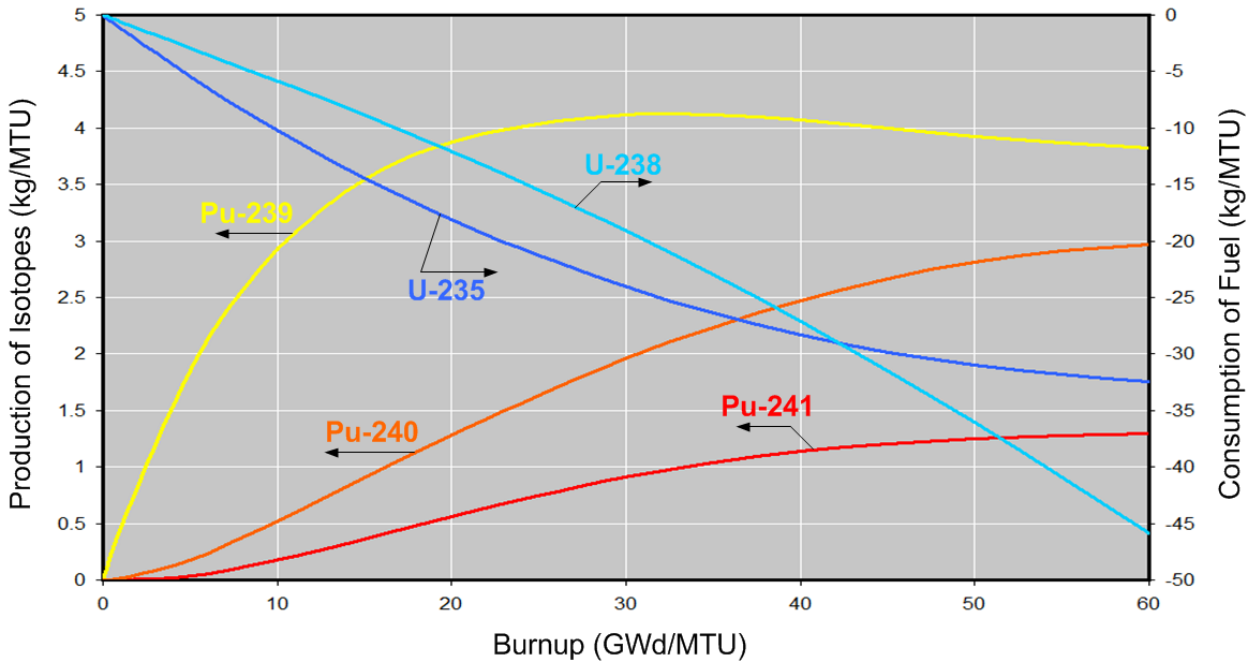

Figure 4.6. AP1000 Production and Consumption of Higher Isotopes.

A more complete tabulation of the actinide transformations within the core is provided in Table 4.4. The mass is given for the actinides produced and consumed at various burnup levels, along with the FPs as a group. Of high importance is the isotopic composition of the TRU produced during the core lifetime as it will become the fuel component for the ABR or the VHTR. The used fuel is very "hot" immediately after removal and must be stored in the onsite reactor cooling pool before being transported to other facilities for reprocessing and fuel fabrication. The reprocessing and fuel fabrication procedures will also involve a substantial amount of time, which translates to a decay/cool-down time period between fuel removal from the AP1000 up to the time the recycled fuel is ready to be used as recycled fuel.

Table 4.4. Nuclide Masses in the AP100 at Different Burnup Levels.

		Average Fuel Burnup (GWd/MTU)									
		0	20	25	30	35	40	45	50	55	60
Mass (kg)	U-234	0.00	0.09	0.10	0.12	0.14	0.16	0.18	0.20	0.23	0.26
	U-235	2920	1309.00	1092.00	851.80	646.00	481.30	349.40	251.50	179.40	127.20
	U-236	0.00	272.20	305.30	340.20	367.70	387.20	399.90	406.30	407.50	405.10
	U-237	0.00	0.54	0.60	0.66	0.75	0.82	0.87	0.92	0.96	0.98
	U-238	83140	82050	81810	81500	81160	80810	80430	80040	79620	79190
	Np-237	0.00	15.08	19.26	24.52	30.03	35.18	40.02	44.28	48.04	51.10
	Pu-238	0.00	2.51	3.86	6.11	8.87	12.04	15.48	18.96	22.36	25.49
	Pu-239	0.00	337.20	347.10	354.20	354.30	350.10	344.30	337.80	333.20	329.10
	Pu-240	0.00	116.40	139.90	168.10	192.30	212.70	229.20	241.80	250.60	255.70
	Pu-241	0.00	51.52	64.46	78.26	89.64	97.80	103.70	107.20	109.70	111.80
	Pu-242	0.00	12.23	19.28	30.83	44.67	60.54	78.38	97.05	116.50	135.70
	Am-241	0.00	0.87	1.23	1.66	2.03	2.28	2.42	2.48	2.50	2.50
	Am-242m	0.00	0.00	0.01	0.01	0.01	0.01	0.01	0.01	0.01	0.01
	Am-243	0.00	1.17	2.21	4.26	7.07	10.67	14.83	19.71	24.83	30.13
	Cm-242	0.00	0.24	0.41	0.69	1.00	1.35	1.67	1.94	2.14	2.28
	Cm-243	0.00	0.00	0.01	0.01	0.02	0.03	0.04	0.05	0.06	0.07
	Cm-244	0.00	0.21	0.50	1.24	2.57	4.73	7.96	12.44	18.40	25.57
	Cm-245	0.00	0.01	0.02	0.05	0.11	0.22	0.40	0.66	1.01	1.44

4.3 VHTR

The results for the VHTR prismatic core were produced by the MCNP code package. Depletion calculations were performed by MCNPX, with core criticality evaluations by MCNP5. The MAKXSF code was used to create temperature dependent neutron cross-section libraries necessary for temperature coefficients of reactivity calculations performed by MCNP5.

The results presented in this section focus on the performance of the VHTR fueled with the recycled TRU from the AP1000 used fuel. Countless possibilities exist for the isotopic composition of the TRU, as they are dependent on control parameters for the AP1000. The VHTR reference case stems from the used AP1000 fuel, which had an initial fuel enrichment of 4.5 wt.%, reached a burnup level of 50 GWd/tIHM, and had a decay/cool-down time of 10 years. The resulting fuel composition for the VHTR is listed in Table 4.5.

The reference VHTR core uses a single batch fuel management scheme. The ENDF/B-VII cross section library was used for fuel temperatures at 1200K and moderator temperatures at 900K. Depletion calculations were performed by MCNPX using 91 day intervals and 600,000 neutron histories per interval.

Table 4.5. Fuel Composition for the VHTR.

Nuclide	Mass (kg)	Weight %
^{237}Np	243.31	4.8301
^{238}Pu	70.86	1.4067
^{239}Pu	2550.57	50.6321
^{240}Pu	1231.89	24.4547
^{241}Pu	376.29	7.4698
^{242}Pu	263.54	5.2316
^{241}Am	247.23	4.9078
^{242m}Am	0.08	0.0017
^{243}Am	42.09	0.8356
^{243}Cm	0.10	0.0020
^{244}Cm	10.67	0.2119
^{245}Cm	0.73	0.0146
^{246}Cm	0.08	0.0015
Total	5037.44	100.0000

Figure 4.7 shows the reactivity as a function of burnup for the VHTR. The k_{eff} at BOC is 1.17 and criticality is maintained up to a burnup level of 264 GWd/tIHM, which equates to a cycle length of 2,220 EFPD. The small reactivity swing and high fuel burnup is the result of many contributing factors, which can be reduced to just a few dominating phenomena. Throughout the core lifetime ^{240}Pu is being converted into the fissile isotope ^{241}Pu at a greater rate than ^{241}Pu is being depleted. In addition, the fissile isotope ^{239}Pu is also being produced by neutron capture in ^{238}Pu, albeit at a slower rate, than it is being destroyed, but the combination of the two (^{241}Pu and ^{239}Pu generation) counteract the depletion of the main fissile component ^{239}Pu, allowing the core to stay above critical for long periods of time. Furthermore, ^{240}Pu comprises a large percentage of the TRU fuel and is also produced by neutron capture in ^{239}Pu throughout core life, which along with the large absorption cross section of ^{240}Pu make it a very effective burnable absorber; effectively limiting the reactivity swing from BOC to EOC.

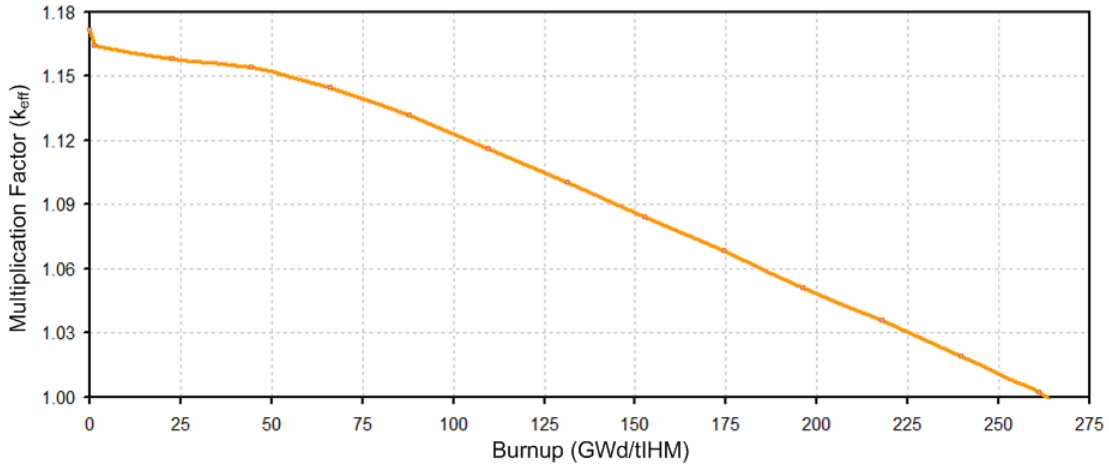

Figure 4.7. VHTR Whole Core Depletion.

The flux profile for different core levels is provided in Figure 4.8.

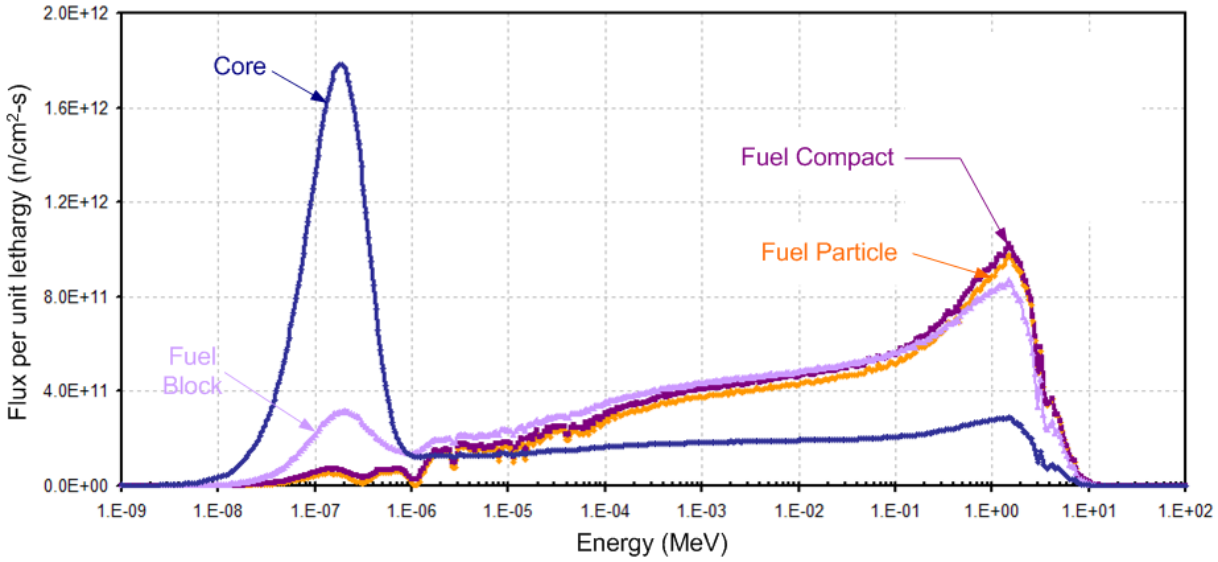

Figure 4.8. VHTR Spectra for Core Regions.

Table 4.6 includes details for TRU consumption/production during the core lifetime. A negative value in the Percent Change (BOC → EOC) column represents consumption, with a positive value indicating production.

Table 4.6. BOC and EOC Fuel Composition for the VHTR.

Nuclide	BOC Initial Loading (kg)	EOC Discharge (kg)	Percent Change BOC → EOC (%)
^{237}Np	243.31	144.70	-40.53
^{238}Pu	70.86	246.90	248.43
^{239}Pu	2550.57	1019.00	-60.05
^{240}Pu	1231.89	1217.00	-1.21
^{241}Pu	376.29	421.30	11.96
^{242}Pu	263.54	302.80	14.90
^{241}Am	247.23	163.50	-33.87
^{242m}Am	0.08	2.12	2452.73
^{243}Am	42.09	70.93	68.51
^{242}Cm	0.00	16.65	na
^{243}Cm	0.10	0.97	852.12
^{244}Cm	10.67	58.69	449.81
^{245}Cm	0.73	9.62	1211.57
^{246}Cm	0.08	0.53	586.88
Pu	4493.14	3207.00	-28.62
TRU	5037.44	3674.71	-27.05

4.4 ABR

The reference ABR core uses a single batch fuel management scheme. Depletion calculations were performed by MCNPX using 50 day intervals and 600,000 neutron histories per interval The charge fuel for the reference case was the same TRU composition as for the VHTR, which is the used fuel from the AP1000 with an initial enrichment of 4.5%, burnup of 50 GWd/tIHM, and 10 years cooling. The TRU composition is listed in Table 4.7. The fuel also consists of 10% Zr and 35% Uranium by weight.

Table 4.7. TRU Fuel Composition for the ABR.

Nuclide	Weight %
^{237}Np	4.8301
^{238}Pu	1.4067
^{239}Pu	50.6321
^{240}Pu	24.4547
^{241}Pu	7.4698
^{242}Pu	5.2316
^{241}Am	4.9078
^{242m}Am	0.0017
^{243}Am	0.8356
^{243}Cm	0.0020
^{244}Cm	0.2119
^{245}Cm	0.0146
^{246}Cm	0.0015
Total	100.0000

Figure 4.9 shows the reactivity as a function of burnup for the ABR. The k_{eff} is 1.11 at BOC and criticality is maintained up to a burnup level of 180 GWd/tIHM.

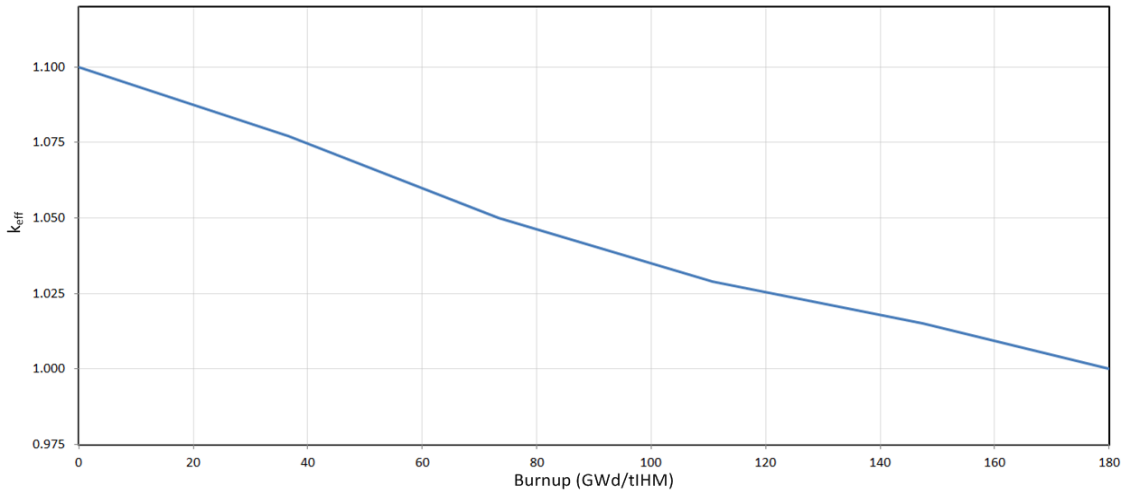

Figure 4.9. ABR Core Depletion.

Table 4.8 list the TRU destruction rates for the ABR. This reference case evaluation did not include multi-cycle operation, which would improve destruction rates.

Table 4.8. BOC and EOC Fuel Composition for the ABR.

Nuclide	BOC Initial Loading (kg)	EOC Discharge (kg)	Percent Change BOC → EOC
^{237}Np	262.39	170.55	-35.00
^{238}Pu	76.42	97.81	28.00
^{239}Pu	2750.55	1347.77	-51.00
^{240}Pu	1328.48	1352.39	1.80
^{241}Pu	405.79	251.59	-38.00
^{242}Pu	284.20	291.59	2.60
^{241}Am	266.61	164.77	-38.20
^{242m}Am	0.09	0.23	145.00
^{243}Am	45.39	46.26	1.90
^{242}Cm	0.00	0.00	na
^{243}Cm	0.11	0.11	-3.20
^{244}Cm	11.51	15.43	34.00
^{245}Cm	0.79	0.73	-8.00
^{246}Cm	0.08	0.08	1.00
Pu	4845.44	3341.16	-31.05
TRU	5432.43	3739.31	-31.17

4.5 Fuel Cycle System Model

The system model couples the individual reactor models and fuel cycle component models together for an effective and time efficient system analysis tool that is capable of accounting for different subsystem input parameters that vary over a range of interest. The computational timesavings are directly related to the treatment of the whole-core 3D depletion models representing the AP100, VHTR, and ABR systems.

The output of the system model includes the following features:

1) TRU mass and composition entering and exiting each subsystem
2) EFPD for reactor systems
3) Fuel burnup levels for reactors (GWd/tIHM)
4) Electricity generation for reactor units (GWd)
5) FP mass and composition entering and exiting each subsystem
6) Uranium mass and composition entering and exiting each subsystem
7) TRU production/destruction rates for reactor units
8) Uranium ore requirements
9) Quantity of UO_2 for system operation
10) DU generated during frontend enrichment procedures
11) Environmental impact measures (energy requirements, CO_2 emissions, water requirements, and land use) per MWh for front-end components
12) Mass, volume, radiotoxicity, and heat load of HLW as a function of time

To illustrate the capabilities a simplified reference case for FC2 was created for simulation. It includes the following input parameters:

- Uranium ore grade 1% U,
- Tail assay 0.3% ^{235}U,
- AP1000 fuel enrichment 3.8%,
- AP1000 thermal efficiency of 32.8%,
- 12 years decay time between AP1000 EOC and VHTR BOC,
- 100% separation procedures during reprocessing,
- Reprocessed TRU becomes fuel component for VHTR,
- TRISO packing fraction of 27%,
- VHTR thermal efficiency of 48%,

A set of selected results for the reference case are listed in Table 4.9.

Table 4.9. Selected System Model Reference Case Results.

Uranium Ore (mine grade 1% U)	73,343 MT
Natural Uranium	735.3 MT
DU stock from enrichment process (0.3% ^{235}U)	647.3 MT
DU recovered from reprocessing (1.5% ^{235}U)	82.42 MT
AP1000-to-VHTR support ratio	4.6

	AP1000 EOC		VHTR EOC	
	Mass (kg)	TRU (w/o)	Mass (kg)	TRU (w/o)
FP	1760		818.1	
^{234}U	0.14		4.78	
^{235}U	950		1.23	
^{236}U	383.3		0.68	
^{238}U	81090		0.0023	
^{237}Np	28.02	4.000	108.88	3.375
^{238}Pu	7.25	1.035	210.69	6.530
^{239}Pu	368.43	52.59	893.28	27.69
^{240}Pu	172.97	24.69	1094.90	33.94
^{241}Pu	82.67	11.80	387.12	12.00
^{242}Pu	32.42	4.628	250.56	7.766
^{244}Pu	0.001	0.00012	0.009	0.00027
^{241}Am	1.898	0.271	143.04	4.434
^{242m}Am	0.010	0.0014	1.795	0.056
^{243}Am	4.610	0.658	60.81	1.885
^{242}Cm	0.774	0.110	16.60	0.515
^{243}Cm	0.013	0.0018	0.981	0.030
^{244}Cm	1.436	0.205	49.29	1.528
^{245}Cm	0.060	0.0085	7.894	0.245
^{246}Cm	0.006	0.00080	0.443	0.014
TRU	700.58	100	3226.3	100
Burnup	32.63 GWd/iTHM		284.9 GWd/iTHM	
EFPD	826		2160	
Elec. Gen.	921.1 GWd		441.2 GWd	

Nuclide	BOC (kg)	EOC (kg)	TRU Production/Destruction (%) (- values indicate destruction)
^{237}Np	188.61	108.88	-42.27
^{238}Pu	47.71	210.69	341.58
^{239}Pu	2431.45	893.28	-63.26
^{240}Pu	1120.48	1094.90	-2.28
^{241}Pu	301.34	387.12	28.46
^{242}Pu	209.81	250.56	19.42
^{244}Pu	0.0054	0.0086	59.77
^{241}Am	245.25	143.04	-41.68
^{242m}Am	0.06	1.80	2839.02
^{243}Am	29.85	60.81	103.75
^{242}Cm	0	16.60	na
^{243}Cm	0.07	0.98	1370.98
^{244}Cm	5.92	49.29	733.21
^{245}Cm	0.39	7.89	1946.49
^{246}Cm	0.04	0.44	1126.57
TRU	4580.97	3226.30	-29.57
Pu	4110.80	2836.57	-31.00

The system model is very useful because it can quickly produce results while also allowing user control over input parameters. The options for system analysis are expanded significantly, as the input variables can take on any value between the defined ranges specified for each. Additionally, when considering the cross-matching between each of the variables, the possible combinations are limitless. As one example, the system model is adjusted so that a ramp function produces input for the AP1000 fuel enrichment. For this case the results as a function of AP1000 fuel enrichment are produced. Figure 4.10 shows how the quantities of ^{239}Pu and ^{240}Pu at the EOC for the VHTR are affected by fuel enrichment changes in the AP1000.

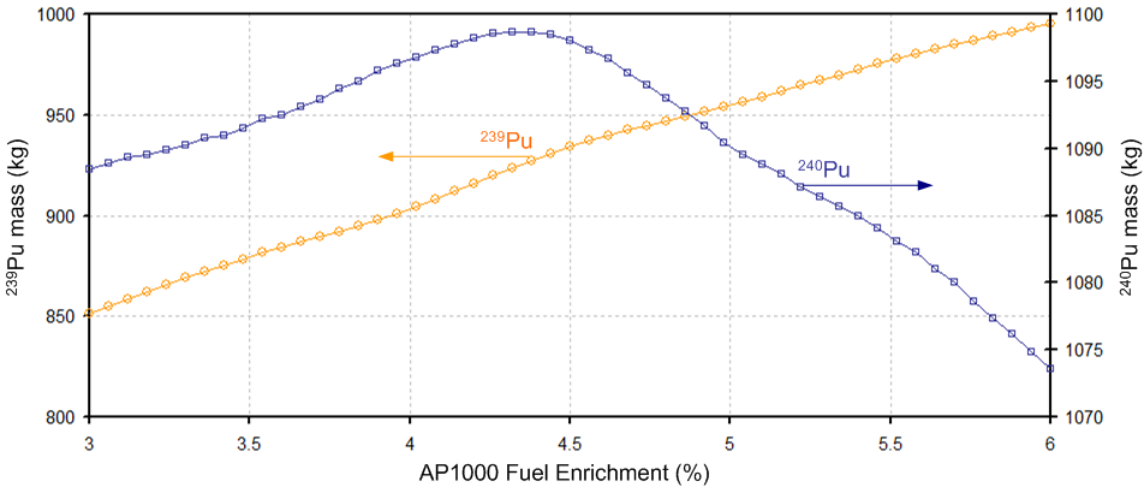

Figure 4.10. VHTR EOC Mass as a Function of AP1000 Fuel Enrichment.

4.6 Sensitivity/Uncertainty Analysis

The capabilities of the fuel cycle model make it possible to assess how variations in input will affect the system on multiple levels. For instance, a change in AP1000 fuel enrichment not only generates enrichment dependent results for the AP1000 system, but it will also affect the results related to other components such as: decay calculations during lag time, irradiation related results for the VHTR and ABR, long-term TRU radiotoxicity calculations for waste management, fuel resource needs for front-end procedures, and front-end environmental measures. Being able to perform such applications and effectively track the results in a time efficient manner allows many possibilities for sensitivity/uncertainty analysis.

The system model was adjusted by setting input parameters to increase by using a ramp function, which allowed for the generation of system wide results as a function of increasing input. Separate cases were performed for each input variable, with the parameter of interest allowed to change while the remaining variables were held constant.

Figure 4.11 provides a diagram of how sensitivity calculations can be performed for FC2. The diagram indicates the inclusion of a ramp function for generating input values for the AP1000 enrichment, with the remaining input ramp functions turned off. The generated output is,

therefore, a function of a linear increasing enrichment value. Additional calculations were performed as the ramp function for each input variable was alternated between on and off.

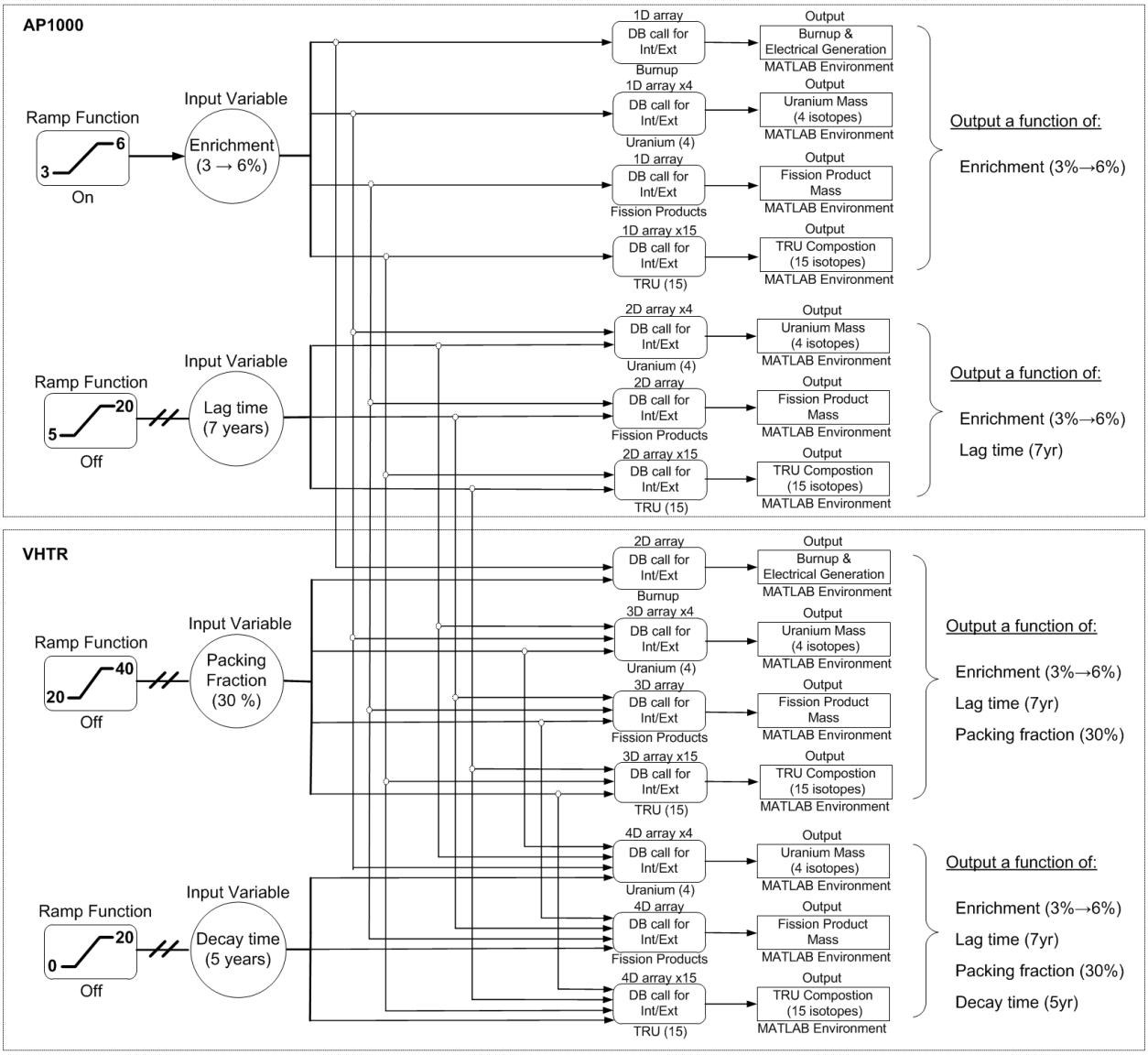

Figure 4.11. Sensitivity Calculations Performed for FC2.

Considering that the input variables have different dimensions and different ranges of values, a non-dimensional sensitivity coefficient was introduced to characterize sensitivity as follows:

$$S_{V_i,X_j} \cong \frac{\partial X_j}{\partial V_i} \cdot \frac{V_i}{X_j} \cong \frac{\delta X_j}{\delta V_i} \cdot \frac{V_i}{X_j}$$

where $S_{Vi,Xj}$ is the non-dimensional sensitivity coefficient, V_i is the *i*th variable, and X_j is the *j*th output variable. A positive/negative sensitivity coefficient $S_{Vi,Xj}$ indicates that output X_j will increase/decrease as the variable V_i increases. The larger the sensitivity coefficient, the larger

effect the variable has on the output. The closer the value is to zero, the less impact the variable has on the output.

The sensitivity coefficients are a useful tool for quickly assessing system behavior, but additional information may be needed to give a complete picture of how the input variables affect the output for the system. The coefficients are only relevant to the end points of the input variables. Therefore, interior behavior might be overlooked, especially if sensitivity is strongly non-linear within the variable range. To account for this possibility plots showing normalized output results as a function of the corresponding input variable can be generated. The slope of the curve indicates the degree of sensitivity, such that the steeper the slope, the greater the sensitivity. A positive slope signifies an increase in the corresponding output variable and a negative slope signifies a decreasing value. An example of this is shown in Figure 4.12, which is a plot of the normalized rate of change for selected U isotopes, FP, TRU destruction, and electricity generation for the ABR as it relates to changes in AP1000 enrichment. The plot provides a useful means of easily comparing the sensitivity of many parameters at once.

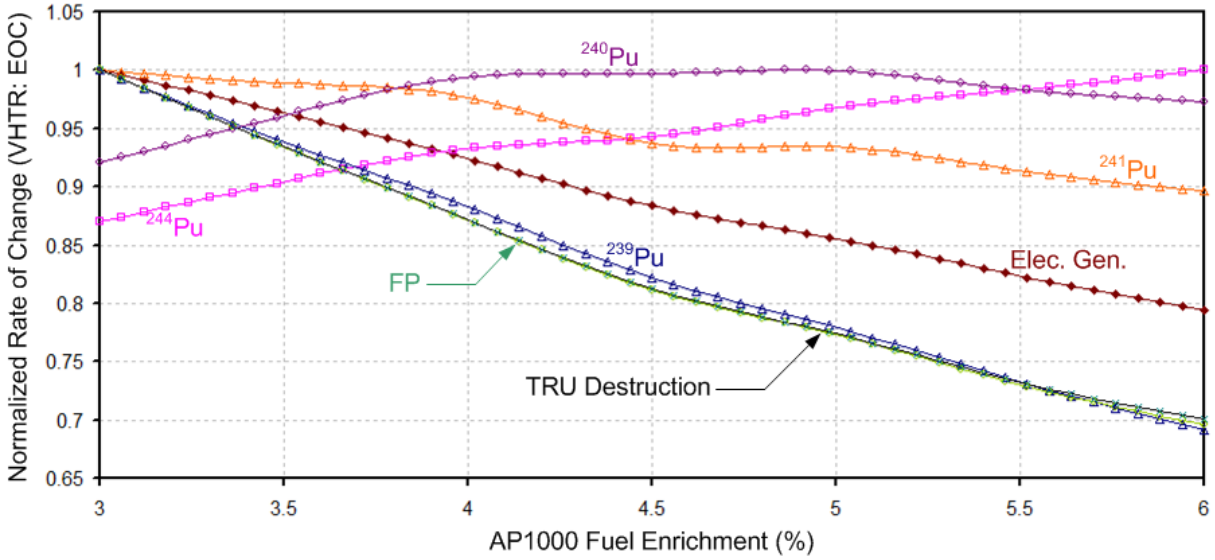

Figure 4.12. Rate of Change for ABR parameters related to AP1000 Enrichment.

4.7 Monte Carlo Based Min/Max Search for Optimization

The conceptual approach for optimization procedures is broken down into the following steps: 1) create a population of random solutions, 2) search for a set of optimum solutions, and 3) select best solution based on criteria preferences.

The population size of random solutions must be large enough to assure that the sampling space accounts for the infinite combinations possible for the input variables. To accomplish this, random number generators are applied to produce input values within the specified range of each input variable. The random number generator assigned to each input variable is unique in its

specified interval and starting seed. One million input values are randomly generated for each variable, thus assuring that the sampling space provides enough random solutions for complete analysis.

The randomly selected input values and subsequently generated solutions are stored within the MATLAB environment, where a subroutine is called to search and retrieve minimum and maximum output values along with their matching input values.

A criteria preference method is used for identifying a single best solution set. The procedure uses a system to weight parameters according to importance relative to final overall system performance goals.

Given that the AP1000 is considered primarily as a means to supply clean, abundant, economic, and safe base load electricity; parameters related to energy production will be weighted heavily. The VHTR is an energy provider, but not on the same scale as the AP1000. The AP1000 generates more than twice the electricity output of the VHTR. Additionally, the support ratio of AP1000 to VHTR is anywhere from 4:1 to 11:1, depending on the input variables used. Therefore, the total electricity generation by the AP1000 is between 8.8 and 24.2 times greater than that for the VHTR. Whereas, the main function of the ABR is to eliminate isotopes that are problematic for long-term HLW management. In a waste management fuel cycle scenario the TRU composition exiting the ABR might outweigh most other parameters. In any case, many possible options exist and must be evaluated in detail.

Considering a fuel cycle where the main goal is to alleviate HLW management issues by targeting the transmutation of TRU the system can be optimized accordingly. A useful measure is the difference in timescale necessary for isolating the HLW from the biosphere for FC1 and FC2. Since long-term effects are targeted, only the radiotoxicity behavior of the TRU is evaluated.

Figure 4.13 show radiotoxicity levels resulting from the irradiated fuel that is removed from the reactor systems in each of the example fuel cycles for a time period extending out to 1 million years. The isotopic activity levels and effective dose coefficients for ingestion $e_{ing}(50)$ [20] are used to produce radiotoxicity measurements. The results in the plot are normalized to the amount of natural uranium from which the HLW originated. The radiotoxicity for the AP1000 is representative of that for a typical PWR and is used as the reference case for the LEU once-through fuel cycle.

The results in Figure 4.13 show that the TRU produced by the AP1000 will remain above the radiotoxicity level of the original uranium ore for at least 100,000 years. The VHTR, which is fueled by the TRU resulting from the AP1000, is effective in destroying a decent fraction of the TRU (particularly the Pu). As a result, the TRU removed from the VHTR reaches uranium ore radiotoxicity levels at 50,000 years. The best case scenario evaluated for the ABR system requires a low conversion ratio with a multi shuffling scheme and fuel reprocessing. The TRU radiotoxicity now drops below uranium ore levels in less than 2,000 years.

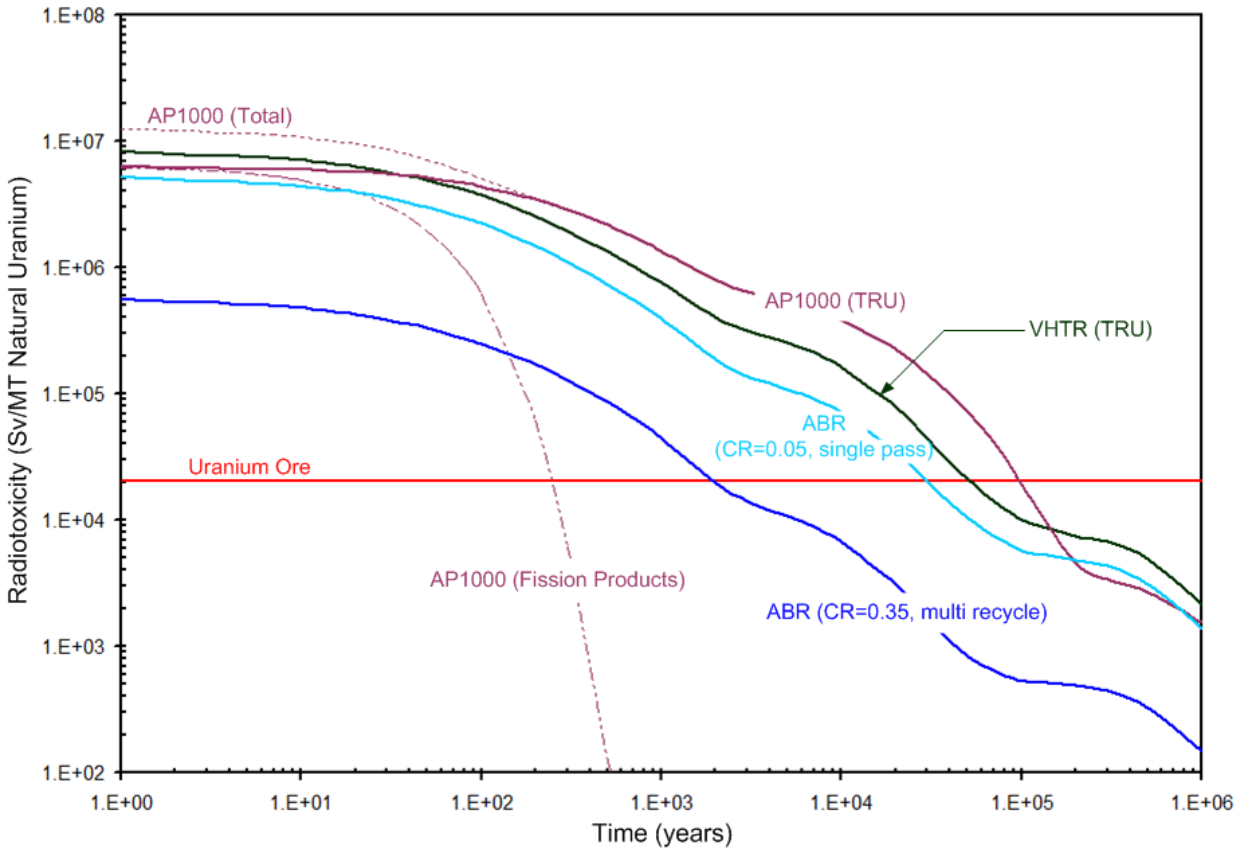

Figure 4.13. TRU Radiotoxicity Measure as a Function of Time.

For even greater time reductions, individual radionuclides can be targeted for destruction in the ABR. Figure 4.14 shows how the major TRU isotopes contribute to the overall radiotoxicity of the TRU produced by the AP1000. Concentrating on strategies to preferentially destroy ^{239}Pu, ^{240}Pu, ^{241}Am, and ^{241}Pu (^{241}Pu because it beta-decays to ^{241}Am) in the ABR can produce even better results, eventually approaching the 300 year limit imposed by the fission products.

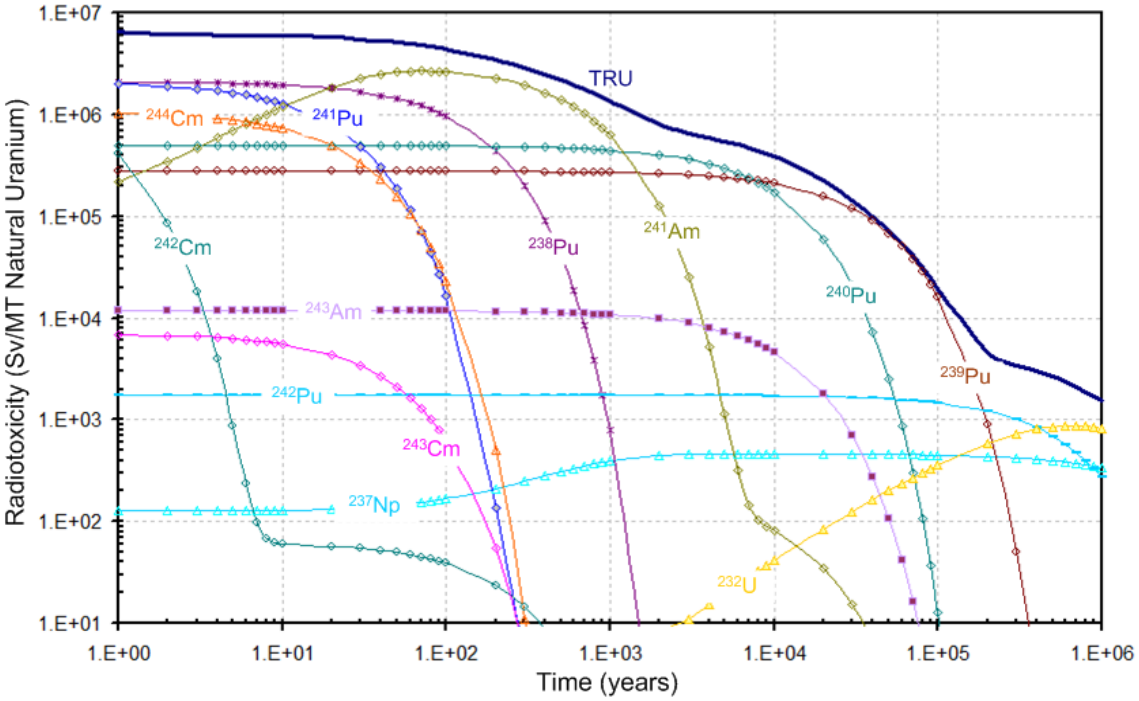

Figure 4.14. Isotopic Radiotoxicity Measure as a Function of Time.

5 CONCLUSIONS

The framework for a fuel cycle system simulation tool has been developed and implemented. The method integrates capabilities of MCNPX for high-fidelity fuel cycle component simulations. The developed computational tool was used to simulate two example fuel cycle options in order to demonstrate capabilities. The analysis takes into account fuel cycle performance characteristics, front-end component environmental impact measures, and the potential effect of used fuel handling on the environment and resource utilization.

Detailed whole-core 3D models were developed for analysis of the individual reactor systems (AP1000, VHTR, ABR). As part of the process, the performance of the models was compared to experiments and independent computational models for benchmarking procedures, which provided substantiation for obtained data and results. Reactor core physics and material depletion calculations were performed and analyzed. Although the reactor models are independent they are coupled by the fuel cycle components and material flows between them.

A computational modeling approach was developed for integrating the individual models. A general approach was utilized allowing for the system model to be modified in order to provide simulation for other systems with similar attributes. By utilizing this approach, it is capable of performing system evaluations under many different design parameter options. The robustness makes it possible to use the same procedure for evaluating advanced fuel cycles that include completely different reactor systems as well.

A method for assessing how variations in key system parameters affect the system on multiple levels was implemented. The results provided valuable information pertaining to system performance that is imperative to gain insight on how subsystem changes can produce unforeseen affects on the overall system. Provided information can be used to assist in implementing design changes for producing system performance aimed at obtaining predetermined global system goals.

The completion of this project has provided the basis for future research that aims to aid in solving the energy crisis that faces future generations, with additional emphasis on addressing environmental concerns.

6 REFERENCES

1. F.M. VANEK, L.D. ALBRIGHT, *Energy Systems Engineering: Evaluation and Implementation*, McGraw-Hill Professional, New York (2008).

2. "Human Development Report 2009: Overcoming Barriers: Human Mobility and Development" Palgrave Macmillan, United Nations Development Program, New York (2009).

3. R. BROGLI, R. KRAKOWSKI, "Degree of Sustainability of Various Nuclear Fuel Cycles," LAUR-01-6939, ISSN 1019-0643, Nuclear Energy and Safety Research Department, Paul Scherrer Institute (2002).

4. P. FINCK, N. EDELSTIEN, Y. ALLEN, C. BURNS, et al., "The Path to Sustainable Nuclear Energy: Basic and Applied Research Opportunities for Advanced Fuel Cycles," Technical Report, Office of Science, U.S. Department of Energy (2005).

5. *MCNP User Manual*, Version 5, LA-UR-03-1987, Vol. I, Los Alamos National Laboratory, Revised (2008).

6. *MCNP User Manual*, Version 5, LA-UR-03-1987, Vol. II, Los Alamos National Laboratory, Revised (2008).

7. D.B. PELOWITZ, Ed., *MCNPX User's Manual*, LA-CP-07-1473, Version 2.6.0, Los Alamos National Laboratory (April 2008).

8. F.B. BROWN, "The MAKXSF Code with Doppler Broadening," Los Alamos National Laboratory Report LA-UR-06-7002, Los Alamos, New Mexico, USA (2006).

9. "SCALE: *A Modular Code System for Performing Standardized Computer Analyses for Licensing Evaluation, Version 6*," ORNL/TM-2005/39, 3 Volumes (January 2009).

10. D.F. HOLLENBACH, L.M. PETRIE, S. GOLUOGLU, N.F. LANDERS, M.E. DUNN, "KENO-VI: A General Quadratic Version of the KENO Program," Vol. II, Sect. F17 of *SCALE*: *A Modular Code System for Performing Standardized Computer Analysis for Licensing Evaluation, Version 6*, ORNL/TM-2005/39, 3 Volumes (January 2009).

11. I.C. GAULD, O.W. HERMANN and R.M. WESTFALL, "ORIGEN-S: SCALE System Module to Calculate Fuel Depletion, Actinide Transmutation, Fission Product Buildup and Decay, and Associated Radiation Source Terms," Vol. II, Sect. F7 of *SCALE: A Modular Code System for Performing Standardized Computer Analyses for Licensing Evaluation, Version 6*, ORNL/TM-2005/39, 3 Volumes (January 2009).

12. "Nuclear Fuel Cycle Simulation System (VISTA)," IAEA-TECDOC-1535, International Atomic Energy Agency, Vienna, Austria (February 2007).

13. MATLAB version 7.9 (R2009b), The MathWorks Inc., Natick, Massachusetts, USA (2009).

14. "Westinghouse AP1000 Design Control Documentation Rev. 16," Tier 2, Chapter 4, Reactor Section 4.3, Nuclear Design. ML071580897 (2007).

15. "Evaluation of High Temperature Gas-cooled Reactor Performance: Benchmark Analysis Related to Initial Testing of the HTTR and HTR-10", IAEA-TECDOC-1382, International Atomic Energy Agency, Vienna, Austria (2003).

16. A. E. Dubberley, K. Yoshida, C. E. Boarman, and T. Wu, "SuperPRISM Oxide and Metal Fuel Cre Designs," Proceedings of ICONE 8, 8th International Conference on Nuclear Engineering (2000).

17. E. A. Hoffman, W. S. Yang, and R. N. Hill, "Preliminary Core Design Studies for the Advanced Burner Reactor over a Wide Range of Conversion Ratios," Argonne National Laboratory, ANL-AFCI-177 (2006).

18. Ferrer, R., M. Asgari, S. Bays, and B. Forget. "Neutronics Methods and Transmutation Performance Analyses for Fast Reactors," Idaho National Laboratory, INL/EXT-07-12466 (2007).

19. Carlsen, Brett, Emily Tavrides, and Erich Schneider. *Measures of the Environmental Footprint of the Front End of the Nuclear Fuel Cycle*. No. INL/EXT-10-20652. Idaho National Laboratory (INL), 2010.

20. "Dose Coefficients for Intakes of Radionuclides by Workers," ICRP Publication 68 in: Annals of the ICRP, Vol. 24, #4, Elsevier Science Inc., Tarrytown, New York (1995).

7 APPENDIX A

HTTR code-to-experiment benchmark supplemental data.

Fuel particle level:

TRISO particle

	material	density (g/cm³)	radius (cm)
Fuel kernel	UO_2	10.41	0.02985
1st coating	PyC	1.14	0.03588
2nd coating	PyC	1.89	0.03895
3rd coating	SiC	3.20	0.04184
4th coating	PyC	1.87	0.04645

Graphite matrix

Material	Density	Impurity
graphite	1.69 g/cm³	0.82 ppm B_{nat}

Unit cell measurements

Volume fraction of grains	Array Pitch	Number of particles per fuel element
0.3	0.1377 cm	176,515

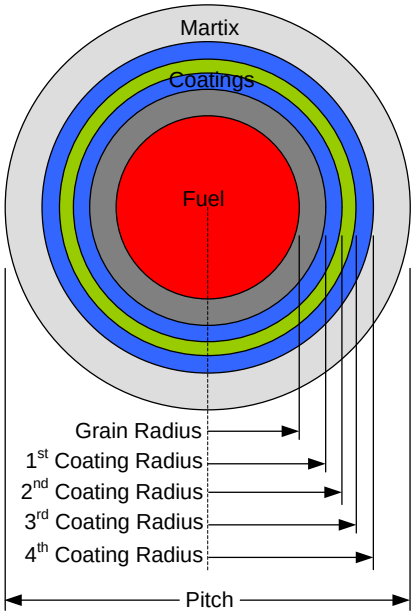

TRISO particle

Fuel element level:

Fuel element properties

Fuel Compact	
Number of fuel particles	176,515
Graphite matrix density	1.690 g/cm³
Graphite matrix Impurity	0.82 ppm B_{nat}
Diameter-inner	1.0 cm
Diameter-outer	2.6 cm
Effective height of fuel rod	54.6 cm

Graphite Sleeve	
Material	Graphite
Density	1.770 g/cm³
Impurity	0.37 ppm B_{nat}
Diameter-inner	2.6 cm
Diameter-outer	3.4 cm
Height	57.7 cm

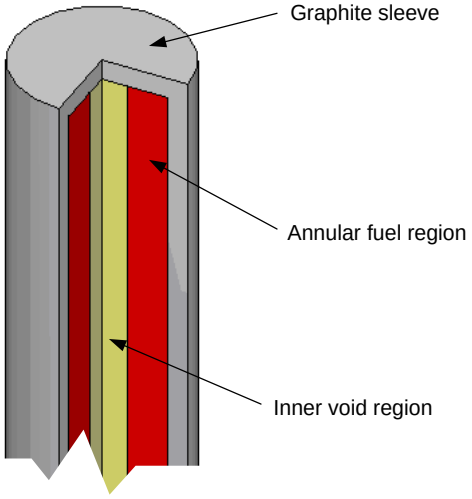

Annular fuel rod

Burnable Poison Rod Properties

Type	H-I	H-II
Absorber section material (2 per rod)	B_4C-C	B_4C-C
Density	1.79 g/cm³	1.82 g/cm³
Natural boron concentration	2.22 wt.%	2.74 wt.%
Diameter	1.39 cm	1.39 cm
Height	20 cm	20 cm
B-10 abundance ratio	18.7 wt.%	18.7 wt.%
Graphite section density	1.77 g/cc	1.77 g/cc
Diameter	1.40 cm	1.40 cm
Height	10 cm	10 cm

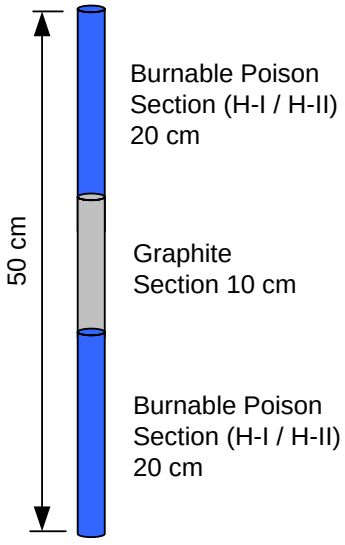

Fuel Assembly Block

Type	Pin-in-block
Configuration	Hexagonal
Material	IG-110 Graphite
Density	1.770 g/cm^3
Impurity	0.40 ppm B_{nat}
Height	58.0 cm
Width across the flats	36.0 cm
Number of fuel holes in block	33 or 31
Fuel hole diameter	4.1 cm
Fuel hole height	58.0 cm
Burnable poison holes	3
Burnable poison hole diameter	1.5 cm
Burnable poison hole height	50.0 cm

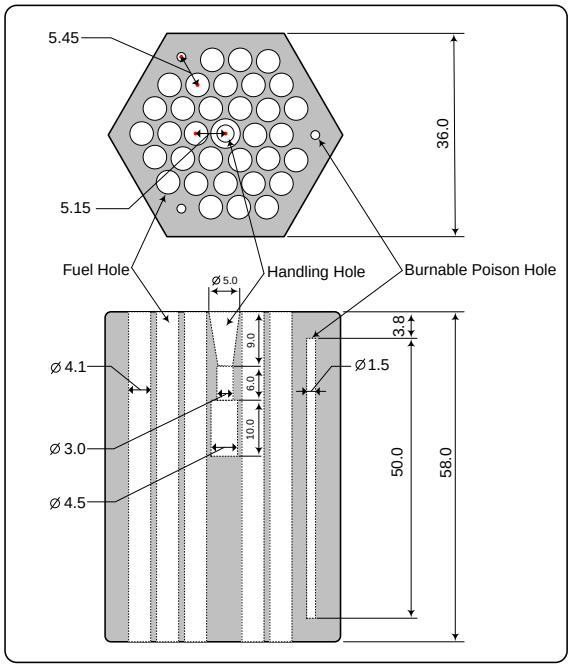

Unit cell measurements

Lattice type	Array Pitch (cm)	Fuel inner radius (cm)	Fuel outer radius (cm)	Sleeve inner radius (cm)	Sleeve outer radius (cm)	Fuel element height (cm)
Triangular	5.15	0.5	1.3	1.3	1.7	54.6

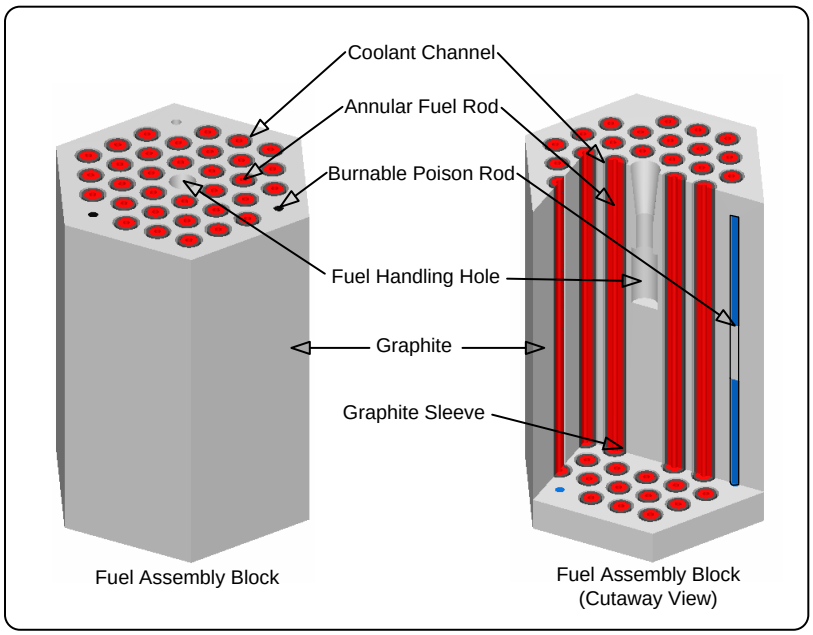

Fuel assembly block with top and quarter section removed to show fuel rods and BP rods.

Control Rod Block and Irradiation Block (irradiation block is identical to control rod block except the holes are used for nuclear instrumentation instead of control rods)

Material	IG-110 Graphite
Density	1.770 g/cm³
Impurity	0.40 ppm B_{nat}
Height	58.0 cm
Width across the flats	36.0 cm
Number control rod holes in block	2
Control rod hole diameter	12.3 cm
Control rod hole height	58.0 cm
Reserve shutdown holes in block	1
Reserve shutdown hole diameter	12.3 cm
Reserve shutdown hole height	58.0 cm

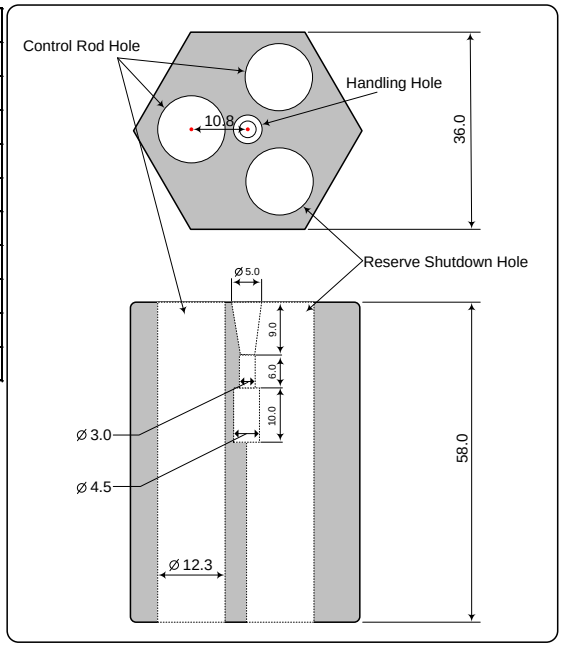

Control Rod Properties

Neutron Absorber Sections (annular)	
Number of neutron absorber sections in each control rod	10
Material	B_4C and C
Density	1.9 g/cm³
Diameter-inner	7.5 cm
Diameter-outer	10.5 cm
Height	29.0 cm
Effective height	290 cm (10 neutron absorber sections)
Spacing between neutron absorber sections	2.2 cm
Control Rod Sleeve	
Material	Alloy 800H
Thickness	0.35 cm
Control Rod	
Number of control rods	32 (16 pairs)
Number of control rods in active core	14 (7 pairs)
Number of control rods in replaceable reflector region	18 (9 pairs)
Diameter-inner	6.5 cm
Diameter-outer	11.3 cm
Height	310 cm

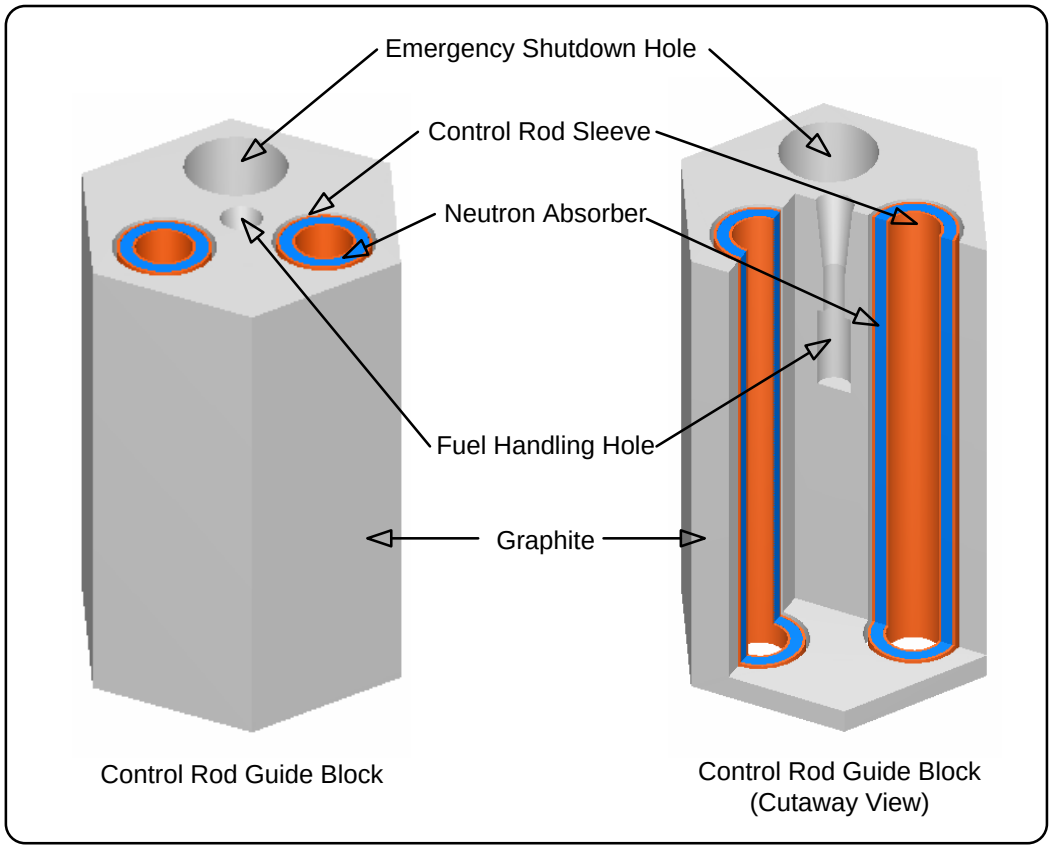

Control rod block with cutaway view

Replaceable Reflector Block (can be solid graphite block or have coolant channels to match the fuel assembly block that it would be associated with)

Configuration	Hexagonal
Material	IG-110 Graphite
Density	1.760 g/cm^3
Impurity	0.37 ppm B_{nat}
Height	58.0 cm
Width across the flats	36.0 cm
Coolant channels (if applicable)	33/31
Coolant hole diameter	4.1 cm
Coolant hole height	58.0 cm

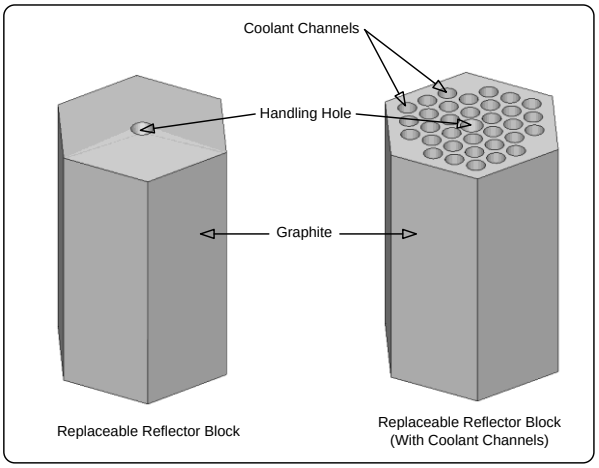

Core Level:

Core Columns

Column	Blocks
Fuel assembly	5 Fuel assembly blocks 4 Reflector blocks (channels)
Reflector	9 Reflector Blocks
Control Rod / Irradiation	9 Control rod blocks

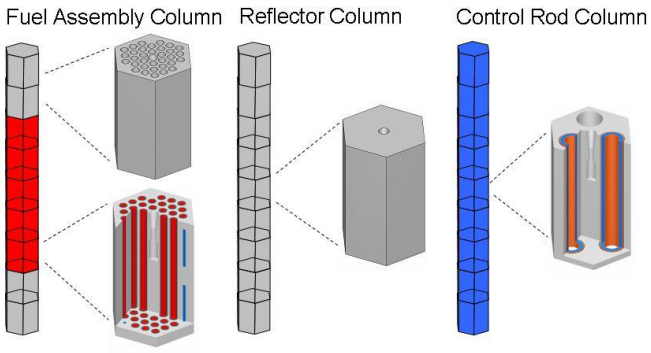

Permanent Reflector Properties

Material	IG-110 Graphite
Density	1.732 g/cm^3
Impurity	2 ppm B_{nat}
Height	522 cm
Radius	215 cm

Overall Core Geometry

	Active core	Whole core
Height	290 cm	522 cm
Radius	115 cm (effective)	215 cm

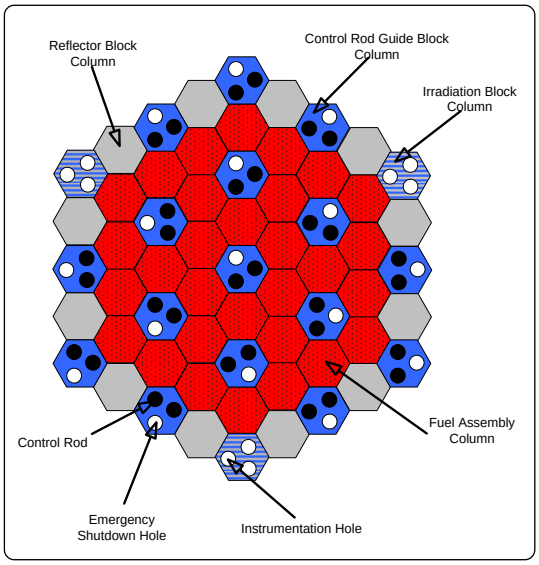

Cross-section core view

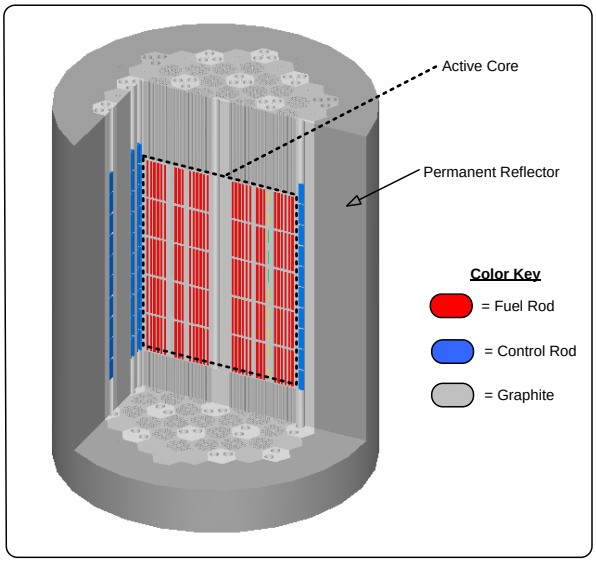

Whole core 3D view

Uranium Enrichments

number	1	2	3	4	5	6	7	8	9	10	11	12
wt. %	3.301	3.864	4.290	4.794	5.162	5.914	6.254	6.681	7.189	7.820	9.358	9.810

Core Arrangement

Layer number from top fuel block	Items	Fuel zone number			
		1	2	3	4
1	Uranium enrichment (wt. %) Number of fuel rods in graphite block Type of burnable poisons	6.681 33 H-I	7.820 33 H-I	9.358 31 H-I	9.810 31 H-I
2	Uranium enrichment (wt. %) Number of fuel rods in graphite block Type of burnable poisons	5.162 33 H-II	6.254 33 H-II	7.189 31 H-II	7.820 31 H-II
3	Uranium enrichment (wt. %) Number of fuel rods in graphite block Type of burnable poisons	4.290 33 H-II	5.162 33 H-II	5.914 31 H-II	6.254 31 H-II
4	Uranium enrichment (wt. %) Number of fuel rods in graphite block Type of burnable poisons	3.301 33 H-I	3.864 33 H-I	4.290 31 H-I	4.794 31 H-I
5	Uranium enrichment (wt. %) Number of fuel rods in graphite block Type of burnable poisons	3.301 33 H-I	3.864 33 H-I	4.290 31 H-I	4.794 31 H-I

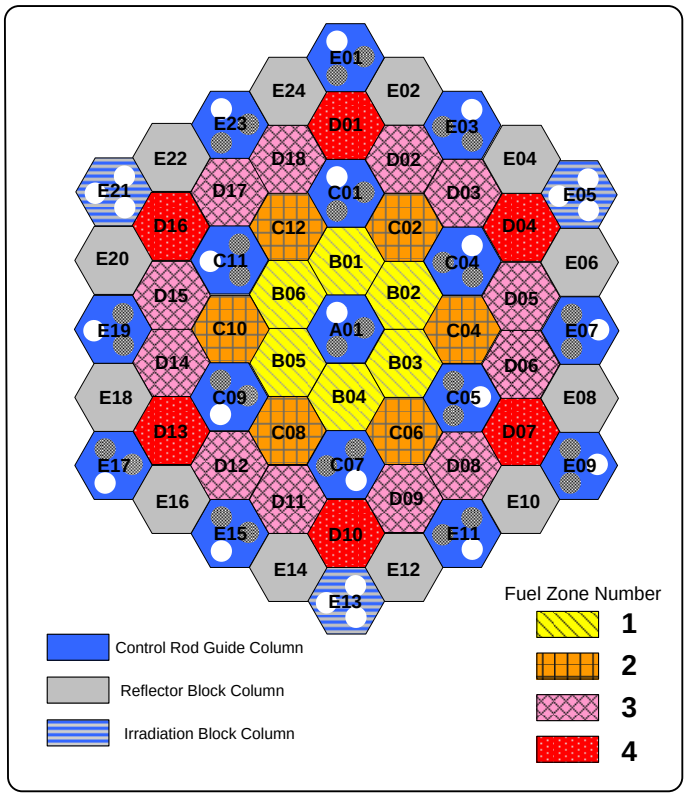

Core Map

Benchmark Results:

Benchmark		VHTR model (calculated)	HTTR (experimental)	Error (%)
Control Rods Fully Withdrawn	k-eff	1.1368 ± 0.0023	1.1363 ± 0.041	0.044
Control Rods Fully Inserted	k-eff	0.6858 ± 0.0019	0.685 ± 0.010	0.117
Critical Insertion Depth (core temperature 300K)	cm	177.1	177.5 ± 0.5	0.225
Critical Insertion Depth (core temperature 418K)	cm	189.9	190.3 ± 0.5	0.210
Temperature Coefficient	dk/k/K	-1.45E-04	-1.42E-04	2.113

8 DISTRIBUTION LIST

1	MS1136	Gary Rochau, 6221
1	MS1136	Tom Lewis, 6221
1	MS1373	Matthew Sternat, 6821
1e	MS0899	Techincal Library, 9536
1e	MS0899	D. Chavez, LDRD Office, 1911

THIS PAGE INTENTIONALLY LEFT BLANK


Sandia National Laboratories